Max-Planck-Institut für Kohlenforschung

Journal article published in: J Comput Aided Mol Des (2016) 30: 989

https://link.springer.com/article/10.1007/s10822-016-9936-x

Calculating distribution coefficients based on multi-scale free energy simulations — An evaluation of MM and QM/MM explicit solvent simulations of water-cyclohexane transfer in the SAMPL5 challenge

Gerhard König[a,b,*], Frank C. Pickard IV[a], Jing Huang[a], Andrew C. Simmonett[a], Florentina Tofoleanu[a], Juyong Lee[a], Pavlo O. Dral[b], Samarjeet[a], Michael Jones[a], Yihan Shao[a], Walter Thiel[b], Bernard R. Brooks[a]

[a] *National Heart, Lung and Blood Institute, Laboratory of Computational Biology, 5635 Fishers Lane, T-900 Suite, Rockville, MD 20852, USA*
[b] *Max-Planck-Institut für Kohlenforschung, 45470 Mülheim an der Ruhr, NRW, Germany, EU*

Abstract

One of the central aspects of biomolecular recognition is the hydrophobic effect, which is experimentally evaluated by measuring the distribution coefficients of compounds between polar and apolar phases. We use our predictions of the distribution coefficients between water and cyclohexane from the SAMPL5 challenge to estimate the hydrophobicity of different explicit solvent simulation techniques. Based on molecular dynamics trajectories with the CHARMM General Force Field, we compare pure molecular mechanics (MM) with quantum-mechanical (QM) calculations based on QM/MM schemes that treat the solvent at the MM level. We perform QM/MM with both density functional theory (BLYP) and semi-empirical methods (OM1, OM2, OM3, PM3). The calculations also serve to test the sensitivity of partition coefficients to solute polarizability as well as the interplay of the quantum-mechanical region with the fixed-charge molecular mechanics environment. Our results indicate that QM/MM with both BLYP and OM2 outperforms pure MM. However, this observation is limited to a subset of cases where convergence of the free energy can be achieved.

*Corresponding author
Email address: gkoenig@mpi-muelheim.mpg.de (Gerhard König)

Keywords: distribution coefficient, partition coefficient, water, cyclohexane, multi-scale free energy simulations, explicit solvent

1. Introduction

The relative solubility of compounds in water and apolar phases is an important element in toxicology, pharmacology and environmental sciences. It also plays a central role in biology in form of the hydrophobic effect, which basically affects all intermolecular interactions in aqueous solution. A classical measure for hydrophobicity is the distribution of compounds between two immiscible phases, such as water and cyclohexane. Therefore, such partition or distribution coefficients can serve as benchmark systems to gauge hydrophobicity of different simulation techniques.

In the most simple case, the partition coefficient P of a compound C is given by

$$\mathrm{P} = \frac{[\mathrm{C}]_{\mathrm{chx}}}{[\mathrm{C}]_{\mathrm{wat}}}, \tag{1}$$

and is based on the respective concentrations [C] in the two phases. This assumes an ideal solution. We use the abbreviations "wat" for water and "chx" for cyclohexane.

The partition coefficient is related to the free energy of transfer between the two phases, $\Delta A_{wat \to chx}$ via

$$\Delta \mathrm{A}_{\mathrm{wat}\to\mathrm{chx}} = -\mathrm{kT} \ln \mathrm{P}, \tag{2}$$

where k is the Boltzmann constant and T is the temperature. Thus, it is often more convenient to use the decadic logarithm of P (rather than P itself), since $\log \mathrm{P}$ is directly proportional to the free energy of transfer, i.e.,

$$\log \mathrm{P} = \frac{-\Delta \mathrm{A}_{\mathrm{wat}\to\mathrm{chx}}}{\mathrm{kT} \ln(10)}. \tag{3}$$

Often the compound does not exist as a single chemical species, but rather in multiple different forms, such as different protonation states, tautomers or multimers. If the experimental determination of the concentrations cannot distinguish between the different species, the result becomes a distribution

coefficient, D, that combines the concentrations of all possible states of the compound in each phase. Thus,

$$D = \frac{\sum_{i=1}^{j} \gamma_i \left[C_i\right]_{chx}}{\sum_{i=1}^{k} \gamma_i \left[C_i\right]_{wat}}, \tag{4}$$

where γ is the activity coefficient and the numbers of possible states (j,k) can also be different in the cyclohexane and the water phase (e.g., the possibility of microsolvation in the apolar phase by dragging water molecules along). Distribution coefficients become most relevant if the compound exists in different protonation states.[1] This aspect makes the distribution coefficients here also realistic benchmark systems for ligand binding, since binding processes are also affected by changes of protonation states.[2] In this context, the apolar phase can be considered a form of homogenous hydrophobic binding pocket.

One of the challenges associated with the computational prediction of distribution coefficients is properly accounting for the change of the solute-solvent electrostatic interactions from a polar to an apolar environment. In nature, the charge distribution of the solute would respond to such changes, but this is not possible in force fields using fixed charges (unless different solute parameters are used in the two phases). One possible way to address this problem is to employ multi-scaling, where molecular mechanics (MM) are combined with quantum-mechanical (QM) methods. Such QM/MM techniques have received increasing attention in the context of free energy calculations,[3–27] starting from the pioneering works of Gao and Warshel,[28–32] and including generalizations and extensions made by others.[33–44] A special focus in that regard is also the development of semi-empirical quantum mechanical methods (SQM),[45–48] which provide a minimalistic description of the QM wave function, leading to a favorable cost/benefit ratio. Recent developments of polarizable force fields also motivate our interest in benchmark systems involving drastic changes of the environment's polarity.[49, 50] By using QM or SQM, the change of the solute charge distribution is accounted for in the postprocessing of the MM trajectories.

In the following, we describe how MM trajectories can be combined with QM/MM and SQM/MM energy functions to obtain partition coefficients for the 53 molecules of the SAMPL5 challenge.[51] This is done by recomputing energies of configurations sampled with MM at the desired QM or SQM

level of theory. Since the individual configurations are independent of each other, these QM/MM and SQM/MM energy calculations are embarrassingly parallel and can be performed on computer clusters with high efficiency. In particular, we focus on the BLYP functional, which has outperformed several other density functional theory methods in recent hydration free energy calculations.[52] Furthermore, we test several semi-empirical methods, including OM1, OM2, OM3 and PM3.[48, 53–56] This provides an assessment of the compatibility of SQM with the MM solvent representations.[57]

The remainder of this paper is organized as follows. We first outline the methods employed in more detail. We then present the results for MM, QM/MM, and various SQM/MM approaches and assess their different performances. For MM and QM/MM, this is done for the complete data set, which was also the basis of our submissions. Since OMx parameters are only available for a subset of the molecules, the corresponding results are discussed separately and were not part of our submissions to the challenge. We compare their differences and critically assess the convergence of the QM/MM results with BLYP and the SQM/MM results from OMx and PM3. The Appendix contains transfer free energy data for other semi-empirical methods such as AM1,[58] MNDO,[59] MNDO/d,[60] and MNDOC[61] as well as dispersion-corrected OM2-D3.[62] A complete description of the QM implicit solvent results, as well as the effect of protonation states on the distribution coefficients is given in a companion paper in the same issue.[63]

2. Methods

We calculated the transfer free energies from water to cyclohexane of the 53 molecules in the SAMPL5 distribution coefficient challenge (see Figure 1).[51] The structures were used exactly as provided by the organizers. No additional calculations were performed to determine tautomeric states of the molecules. Only the neutral, uncharged form of each molecule was used (the effect of pK_a predictions are considered in our companion paper).[63] The SAMPL challenges[22, 41, 64–82] have emerged as a central venue for computational chemists to compare their methods based on blinded, high quality experimental data, and are therefore an ideal framework for our evaluation of MM, QM/MM and SQM/MM. Each transfer free energy was calculated with the standard thermodynamic cycle.[83–87] The calculation of the transfer free energy from water to cyclohexane ($\Delta A_{wat \rightarrow chx}$) consisted of four steps: First, the charges of the solute were gradually turned off in wa-

Figure 1: Structures of the 53 molecules involved in the SAMPL5 distribution coefficient challenge.

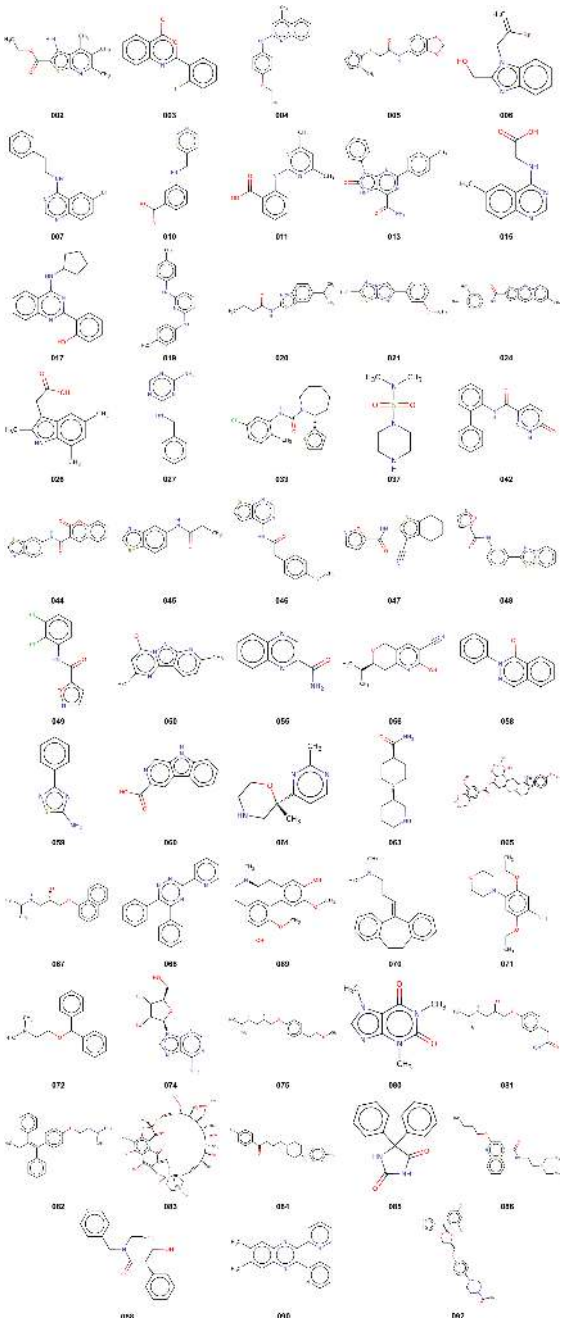

Figure 2: Thermodynamic cycle to calculate the transfer free energy from water (wat) to cyclohexane (chx). In each leg of the cycle, the solute is turned into an uncharged solute, followed by removing the van der Waals interactions, which turns the solute into a dummy molecule.

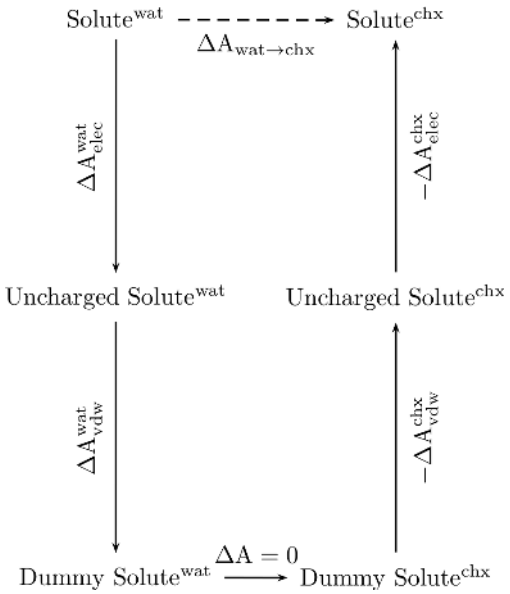

ter (ΔA^{wat}_{elec}). Second, the uncharged solute was mutated to dummy atoms without any non-bonded interactions (ΔA^{wat}_{vdw}). This state corresponds to a dummy molecule in the gas phase plus the aqueous environment. Third and fourth, the analogous steps were carried out in the cyclohexane phase (ΔA^{chx}_{elec} and ΔA^{chx}_{vdw}). Thus, each water-cyclohexane transfer free energy was calculated according to:

$$\Delta A_{wat\rightarrow chx} = \Delta A^{wat}_{elec} + \Delta A^{wat}_{vdw} - \Delta A^{chx}_{vdw} - \Delta A^{chx}_{elec} \quad (5)$$

The corresponding thermodynamic cycle is depicted in Figure 2.

2.1. MM simulations

All free energy calculations were conducted with CHARMM,[88, 89] using the CHARMM General Force Field (CGenFF) for organic molecules.[90] The MM free energy differences were computed with Bennett's Acceptance ratio method.[91] In all aqueous solvent simulations 1906 TIP3P water molecules[92,

93] were present. To approximately reproduce the ionic strength of the reported experimental conditions (ca. pH 7.6, 136 mM NaCl, 2.6 mM KCl, 7 mM Na_2PO_4, 1.46 mM KH_2PO_4 plus 0.27 M DMSO and 0.18 M acetonitrile), six sodium and six chlorine ions were added to the water box. The simulation boxes were cubes with side lengths between 38.55 and 38.75 Å, which was the average box size from 0.5 ns of constant pressure simulations. The corresponding apolar phase simulations included 337 cyclohexane molecules with box sizes between 39.93 and 40.18 Å. A Nosé-Hoover thermostat was used to keep the temperature at 300 K. Long range electrostatic interactions were computed with the Particle Mesh Ewald method [94] and Lennard-Jones interactions were switched off between 10 and 12 Å. All molecules were first equilibrated for 0.5 ns using constant pressure, followed by an equilibration of each λ alchemical transformation state for 0.5 ns using constant volume. Production simulations of each phase were conducted for 5 ns. All simulations used a time step of 1 fs, saving frames every 1000 steps. SHAKE[95] was used to keep all bonds involving hydrogens in the solvent rigid. To ensure proper sampling of all relevant solute degrees of freedom, λ-Hamiltonian Replica Exchange [96] was employed to exchange structures between neighboring λ points every 1000 steps. Standard deviations were calculated from ten block averages of 500 frames each.

The free energy simulations in each phase were divided into 32 λ states. ΔA_{elec} was calculated in five steps, where the charges were scaled by factors of 1.00, 0.90, 0.75, 0.50, 0.25, and 0.00. ΔA_{vdw} was calculated by turning off the van der Waals interactions in 23 equidistant steps (λ=1.0,0.957,...,0.0435,0.0). For molecules 65, 83 and 92 an additional point at λ=0.022 was necessary to achieve converged results. Soft cores, as implemented with the PSSP command in the PERT module of CHARMM, were used with the default parameters to avoid the end point problem.[88, 97]

2.2. QM/MM and SQM/MM corrections

The QM/MM potential energy calculations were performed with Q-Chem[98] driven by the CHARMM/Q-Chem interface.[99] SQM/MM potential energy evaluations were performed with a local version of the MNDO program.[100] Electrostatic embedding was used (i.e., the QM or SQM solute is polarized by the MM point charges of the solvent, but the solute-solvent van der Waals interactions are still calculated on the MM level). The MM→(S)QM/MM free energy corrections were computed with the Zwanzig equation (also known as Free Energy Perturbation or the Exponential Formula).[101] The Zwanzig

equation was chosen here because of restricted computational resources and because recent work indicates that the limiting factor for multi-scale free energy simulations is not the free energy method, but rather the phase space overlap between MM and QM.[102, 103] In particular, five different methods were evaluated: a) the density-functional theory method BLYP[104, 105] with the 6-31G* basis set, and four semi-empirical methods b) OM1,[48, 53] c) OM2,[48, 54] d) OM3,[48, 55] and e)PM3.[56]

To obtain transfer free energies, the MM transfer free energy was combined with QM/MM and SQM/MM corrections,

$$\Delta A^{x}_{wat\rightarrow chx} = \Delta A^{MM}_{wat\rightarrow chx} + \Delta\Delta A^{x}_{correction} \ , \tag{6}$$

where x represents the corresponding QM or SQM method. Only the solute was treated with QM or SQM, while the solvent was represented by MM point charges. The correction was calculated from the free energy difference between MM and QM in cyclohexane, $\Delta A^{MM\rightarrow x}_{solu,chx}$, and in water, $\Delta A^{MM\rightarrow x}_{solu,wat}$, i.e. $\Delta\Delta A^{x}_{correction} = \Delta A^{MM\rightarrow x}_{solu,chx} - \Delta A^{MM\rightarrow x}_{solu,wat}$.

3. Results and Discussion

The transfer free energies from water to cyclohexane for the 53 molecules of the SAMPL5 distribution coefficient challenge based on CGenFF[90] are reported in Table 1. The presented data corresponds to our submission number 26. The table also includes the pathway-dependent van der Waals contributions (second column) and electrostatic contributions (third column) to the transfer free energy, as well as the corresponding logP values (fourth column). The experimental logD reference data are given in the rightmost column. The coefficient of determination (R^2), mean signed deviation (MSD), mean absolute deviation (MAD) and root mean square deviation (RMSD) from the experimental results are given in the last four rows of the table, both in terms of the free energies (kcal/mol) on the left, and in terms of logP (unitless) on the right.

The RMSD of the CGenFF results (4.4 kcal/mol) is almost twice as high as the corresponding RMSD for hydration free energies (2.3 kcal/mol)[41] or binding free energies (2.6 kcal/mol)[72] of the same force field in previous challenges. Thus the deviation is higher than what could be expected from error propagation, if one assumes that both the water and the cyclohexane phase exhibit the same error as the SAMPL4 hydration free energy results

Table 1: Transfer free energies and their components (in kcal/mol), as well as partition coefficients from water to cyclohexane based on CGenFF.

Mol [a]	ΔA_{vdw} [b]	ΔA_{elec} [c]	$\Delta A^{MM}_{wat\rightarrow chx}$ [d]	$logP^{MM}$ [e]	$logD^{exp}$ [f]
2	-13.4 ± 0.1	9.3 ± 0.2	-4.0 ± 0.2	3.0 ± 0.2	1.4
3	-11.8 ± 0.1	7.9 ± 0.1	-4.0 ± 0.2	2.9 ± 0.1	1.9
4	-15.2 ± 0.2	9.4 ± 0.1	-5.8 ± 0.2	4.3 ± 0.1	2.2
5	-14.8 ± 0.2	16.9 ± 0.1	2.1 ± 0.3	-1.6 ± 0.2	-0.9
6	-11.5 ± 0.1	13.4 ± 0.1	1.9 ± 0.2	-1.4 ± 0.1	-1.0
7	-14.3 ± 0.3	8.6 ± 0.5	-5.7 ± 0.6	4.2 ± 0.4	1.4
10	-11.9 ± 0.1	14.1 ± 0.2	2.3 ± 0.2	-1.7 ± 0.1	-1.7
11	-12.9 ± 0.1	14.4 ± 0.2	1.5 ± 0.2	-1.1 ± 0.2	-3.0
13	-17.5 ± 0.2	23.4 ± 0.4	6.0 ± 0.5	-4.4 ± 0.3	-1.5
15	-11.4 ± 0.2	12.6 ± 0.2	1.2 ± 0.3	-0.9 ± 0.2	-2.2
17	-16.0 ± 0.2	6.9 ± 0.3	-9.1 ± 0.4	6.6 ± 0.3	2.5
19	-15.9 ± 0.2	12.4 ± 0.1	-3.5 ± 0.2	2.5 ± 0.1	1.2
20	-13.9 ± 0.2	16.5 ± 0.5	2.6 ± 0.6	-1.9 ± 0.4	1.6
21	-12.7 ± 0.1	10.7 ± 0.1	-2.0 ± 0.2	1.5 ± 0.1	1.2
24	-17.6 ± 0.3	10.5 ± 0.1	-7.1 ± 0.3	5.2 ± 0.2	1.0
26	-12.3 ± 0.1	10.0 ± 0.2	-2.3 ± 0.2	1.7 ± 0.2	-2.6
27	-10.7 ± 0.1	9.1 ± 0.1	-1.6 ± 0.2	1.2 ± 0.1	-1.9
33	-16.6 ± 0.3	9.2 ± 0.1	-7.4 ± 0.3	5.4 ± 0.2	1.8
37	-9.1 ± 0.2	11.4 ± 0.1	2.3 ± 0.2	-1.7 ± 0.1	-1.5
42	-9.6 ± 1.0	17.8 ± 0.2	8.1 ± 1.1	-6.0 ± 0.8	-1.1
44	-15.6 ± 0.2	10.7 ± 0.1	-4.8 ± 0.2	3.6 ± 0.1	1.0
45	-10.8 ± 0.1	13.8 ± 0.1	3.0 ± 0.1	-2.2 ± 0.1	-2.1
46	-15.9 ± 0.2	12.8 ± 0.7	-3.1 ± 0.7	2.3 ± 0.5	0.2
47	-13.7 ± 0.2	13.6 ± 0.1	-0.1 ± 0.2	0.1 ± 0.1	-0.4
48	-9.6 ± 0.2	13.1 ± 0.1	3.5 ± 0.3	-2.6 ± 0.2	0.9
49	-6.5 ± 0.2	7.6 ± 0.1	1.0 ± 0.2	-0.7 ± 0.1	1.3
50	-11.4 ± 0.1	12.8 ± 0.1	1.4 ± 0.2	-1.0 ± 0.1	-3.2
55	-9.0 ± 0.2	7.9 ± 0.1	-1.1 ± 0.2	0.8 ± 0.2	-1.5
56	-11.7 ± 0.2	10.8 ± 0.2	-0.9 ± 0.2	0.7 ± 0.2	-2.5
58	-11.7 ± 0.1	15.4 ± 0.1	3.7 ± 0.2	-2.7 ± 0.1	0.8
59	-9.2 ± 0.1	8.1 ± 0.1	-1.1 ± 0.1	0.8 ± 0.1	-1.3
60	-10.7 ± 0.1	16.1 ± 0.1	5.4 ± 0.1	-3.9 ± 0.1	-3.9
61	-10.1 ± 0.1	9.5 ± 0.2	-0.7 ± 0.2	0.5 ± 0.2	-1.5
63	-9.8 ± 0.1	11.5 ± 0.1	1.8 ± 0.2	-1.3 ± 0.1	-3.0
65	-26.8 ± 0.3	28.4 ± 0.1	1.6 ± 0.4	-0.7 ± 0.3	0.7
67	-13.8 ± 0.2	8.4 ± 0.1	-5.4 ± 0.2	4.0 ± 0.1	-1.3
68	-16.2 ± 0.2	14.7 ± 0.1	-1.5 ± 0.2	1.1 ± 0.1	1.4
69	-15.7 ± 0.4	11.5 ± 0.1	-4.2 ± 0.4	3.1 ± 0.3	-1.3
70	-15.4 ± 0.2	6.3 ± 0.0	-9.1 ± 0.2	6.7 ± 0.1	1.6
71	-14.4 ± 0.4	13.2 ± 0.1	-1.2 ± 0.4	0.9 ± 0.3	-0.1
72	-14.3 ± 0.3	7.6 ± 0.1	-6.7 ± 0.3	4.9 ± 0.2	0.6
74	-7.9 ± 0.2	22.0 ± 0.2	14.1 ± 0.3	-10.3 ± 0.2	-1.9
75	-15.4 ± 0.2	10.6 ± 0.1	-4.7 ± 0.2	3.5 ± 0.2	-2.8
80	-10.1 ± 0.1	18.8 ± 0.1	8.7 ± 0.1	-6.3 ± 0.1	-2.2
81	-14.4 ± 0.2	17.1 ± 0.1	2.7 ± 0.2	-2.0 ± 0.1	-2.2
82	-20.3 ± 0.3	8.7 ± 0.1	-11.5 ± 0.3	8.4 ± 0.2	2.5
83	-23.6 ± 0.7	28.3 ± 0.4	4.8 ± 0.9	-3.3 ± 0.7	-1.9
84	-17.7 ± 1.6	15.1 ± 0.1	-2.6 ± 1.6	1.9 ± 1.2	0.0
85	-12.8 ± 0.2	22.6 ± 0.1	9.8 ± 0.2	-7.2 ± 0.1	-2.2
86	-19.3 ± 0.2	8.9 ± 0.1	-10.3 ± 0.2	7.6 ± 0.2	0.7
88	-15.0 ± 0.2	20.7 ± 0.2	5.8 ± 0.3	-4.2 ± 0.2	-1.9
90	-15.8 ± 0.3	12.3 ± 0.5	-3.5 ± 0.6	2.6 ± 0.5	0.8
92	-23.4 ± 0.2	25.8 ± 0.3	2.4 ± 0.3	-1.7 ± 0.2	-0.4
			(kcal/mol)	(log)	
R^2 [g]	**0.1**	**0.1**	**0.3**	**0.3**	
MSD [h]			**-1.2**	**0.9**	
MAD [i]			**3.6**	**2.6**	
RMSD [j]			**4.4**	**3.3**	

[a] Molecule number [b] Pathway-dependent van der Waals contribution to the transfer free energy ($\Delta A^{wat}_{vdw} - \Delta A^{chx}_{vdw}$) [c] Pathway-dependent electrostatic contribution to the transfer free energy ($\Delta A^{wat}_{elec} - \Delta A^{chx}_{elec}$)

[d] Transfer free energy from water to cyclohexane [e] Partition coefficient $-\Delta A_{wat\rightarrow chx}/(2.303\ kT)$ [f] Experimental distribution coefficient results [g] Coefficient of determination with respect to experimental logD [h] Mean signed deviation from experimental logD results [i] Mean absolute deviation from experimental logD results [j] Root mean square deviation from experimental logD results

($\sqrt{2 \times 2.3^2}$ = 3.3 kcal/mol). While the MSE of CGenFF in the SAMPL4 hydration free energy challenge was negligible (0.02 kcal/mol), the MSE here is −1.2 kcal/mol. This indicates that the affinity for the apolar phase is systematically overestimated, or that the affinity for water is systematically underestimated (or both). Since the hydration free energy results in SAMPL4 did not exhibit a systematic error, it is more likely that the systematic error arises in the apolar phase. However, since different molecules were used in the two challenges this might also be an apparent effect of the data sets. The standard deviations are on average 0.3 kcal/mol and lie for most molecules below 0.5 kcal/mol. The only exceptions are molecules 7, 20, 42, 46, 83, 84 and 90. The increased standard deviations for those molecules indicate either sampling issues or insufficient overlap between some of the λ points.

The transfer free energy depends on the balance between a) cavity formation (which corresponds to the strength of the solvent–solvent interactions), b) solute-solvent van der Waals interactions, and c) electrostatic solute–solvent interactions. The van der Waals contribution to the transfer free energy (ΔA_{vdw}, second column) combines the first two effects and, in all cases, favors the apolar phase (ΔA between −27.4 and −6.5 kcal/mol). This indicates that cavity formation is easier in cyclohexane than in water, and/or that the solute–solvent dispersion forces are stronger in the apolar phase. Since the CHARMM cyclohexane parameters reproduce the experimental enthalpy of vaporization to ca. 0.4 kcal/mol (or 5%),[90] and the TIP3P water model to ca. 0.3 kcal/mol (3%)[106] it can be assumed that the solvent–solvent interactions are adequate in both phases (unless the models significantly misrepresent the solvent entropy). Thus, the major unknown here is whether the solute–solvent dispersion interactions exhibit the correct balance in the two phases.

The electrostatic contributions (ΔA_{elec}, third column) in all cases favor the aqueous phase, which is of course related to the higher polarity of water. It is possible that the usage of the same set of pre-polarized point charges in both the polar and the apolar phase artificially increases lipophilicity. Since the solute point charges were primarily generated with solute–water interactions in mind, they might be too high for the apolar phase. If that is the case, the problem might be mitigated by the use of polarizable force fields or quantum-mechanical methods.

To illustrate the effect of making the solute charges dependent on the environment, multi-scale free calculations were performed with BLYP/6-31G* based on the CGenFF trajectories. The corresponding results are shown in

Table 2: Transfer free energies and their components (in kcal/mol) as well as partition coefficients from water to cyclohexane based on QM/MM with BLYP.

Mol[a]	$\Delta A_{solu,wat}^{MM\rightarrow BLYP}$ [b]	$\Delta A_{solu,chx}^{MM\rightarrow BLYP}$ [c]	$\Delta\Delta A_{corr}^{BLYP}$ [d]	$\Delta A_{wat\rightarrow chx}^{BLYP}$ [e]	$LogP^{BLYP}$ [f]	$LogD^{exp}$ [g]
2	-729809.5 ± 1.3	-729807.9 ± 1.2	1.6 ± 1.8	-2.5 ± 1.8	1.8 ± 1.3	1.4
3	-529059.2 ± 0.5	-529059.7 ± 1.3	-0.5 ± 1.4	-4.5 ± 1.4	3.3 ± 1.0	1.9
4	-552895.4 ± 1.6	-552895.1 ± 1.4	0.3 ± 2.1	-5.5 ± 2.1	4.0 ± 1.5	2.2
5	-810073.0 ± 1.1	-810076.4 ± 1.6	-3.3 ± 2.0	-1.2 ± 2.0	0.9 ± 1.5	-0.9
6	-1998151.6 ± 0.4	-1998150.1 ± 0.4	1.5 ± 0.6	3.3 ± 0.6	-2.4 ± 0.4	-1.0
7	-2105885.0 ± 4.4	-2105876.2 ± 1.6	8.8 ± 4.7	3.1 ± 4.7	-2.2 ± 3.5	1.4
10	-478361.5 ± 1.1	-478360.8 ± 2.3	0.7 ± 2.5	3.0 ± 2.5	-2.2 ± 1.8	-1.7
11	-512901.7 ± 2.0	-512896.3 ± 0.8	5.3 ± 2.2	6.8 ± 2.2	-5.0 ± 1.6	-3.0
13	-725961.8 ± 4.0	-725959.3 ± 1.3	2.4 ± 4.2	8.4 ± 4.2	-6.1 ± 3.1	-1.5
15	-464483.0 ± 1.2	-464480.7 ± 1.7	2.4 ± 2.1	3.6 ± 2.1	-2.6 ± 1.6	-2.2
17	-611516.9 ± 0.8	-611517.3 ± 0.7	-0.3 ± 1.1	-9.4 ± 1.1	6.9 ± 0.8	2.5
19	-574305.2 ± 1.7	-574305.9 ± 1.4	-0.6 ± 2.2	-4.1 ± 2.2	3.0 ± 1.6	1.2
20	-707104.0 ± 0.6	-707111.6 ± 0.7	-7.5 ± 0.9	-4.9 ± 1.1	3.6 ± 0.8	1.6
21	-691097.2 ± 0.8	-691096.4 ± 1.0	0.8 ± 1.3	-1.2 ± 1.3	0.8 ± 0.9	1.2
24	-874551.2 ± 1.4	-874543.9 ± 0.7	7.4 ± 1.6	0.3 ± 1.6	-0.2 ± 1.2	1.0
26	-445069.9 ± 1.3	-445065.9 ± 0.7	4.0 ± 1.5	1.6 ± 1.5	-1.2 ± 1.1	-2.6
27	-414520.4 ± 0.9	-414514.9 ± 0.5	5.5 ± 1.1	3.9 ± 1.1	-2.9 ± 0.8	-1.9
33	-1092646.1 ± 0.9	-1092641.9 ± 1.2	4.2 ± 1.5	-3.2 ± 1.5	2.4 ± 1.1	1.8
37	-596312.1 ± 0.6	-596312.1 ± 0.6	0.0 ± 0.8	2.3 ± 0.9	-1.7 ± 0.6	-1.5
42	-608725.2 ± 1.9	-608723.2 ± 1.4	2.0 ± 2.4	10.2 ± 2.6	-7.4 ± 1.9	-1.1
44	-870266.6 ± 1.4	-870264.4 ± 1.5	2.2 ± 2.1	-2.6 ± 2.1	1.9 ± 1.6	1.0
45	-608513.4 ± 0.5	-608513.7 ± 0.3	-0.3 ± 0.6	2.7 ± 0.6	-2.0 ± 0.4	-2.1
46	-1013354.8 ± 1.4	-1013351.3 ± 1.0	3.5 ± 1.7	0.3 ± 1.8	-0.3 ± 1.3	0.2
47	-762167.7 ± 0.7	-762166.2 ± 0.8	1.5 ± 1.1	1.4 ± 1.1	-1.0 ± 0.8	-0.4
48	-857854.9 ± 0.9	-857854.7 ± 1.2	0.2 ± 1.5	3.7 ± 1.6	-2.7 ± 1.1	0.9
49	-981931.5 ± 1.6	-981927.9 ± 0.4	3.6 ± 1.6	4.6 ± 1.7	-3.4 ± 1.2	1.3
50	-451272.4 ± 1.6	-451271.4 ± 2.3	1.0 ± 2.8	2.4 ± 2.8	-1.8 ± 2.1	-3.2
55	-368124.4 ± 1.4	-368119.3 ± 1.0	5.0 ± 1.7	3.9 ± 1.7	-2.9 ± 1.3	-1.5
56	-455139.7 ± 3.0	-455130.7 ± 0.6	9.0 ± 3.0	8.1 ± 3.0	-5.9 ± 2.2	-2.5
58	-454343.0 ± 0.6	-454348.8 ± 1.2	-5.8 ± 1.3	-2.1 ± 1.3	1.5 ± 0.9	0.8
59	-546783.4 ± 1.6	-546780.0 ± 0.9	3.4 ± 1.8	2.3 ± 1.8	-1.7 ± 1.3	-1.3
60	-453012.0 ± 1.0	-453009.7 ± 0.4	2.3 ± 1.1	7.6 ± 1.1	-5.6 ± 0.8	-3.9
61	-394855.5 ± 1.9	-394853.2 ± 0.8	2.3 ± 2.1	1.7 ± 2.1	-1.2 ± 1.5	-1.5
63	-421029.2 ± 0.9	-421023.3 ± 0.8	5.9 ± 1.2	7.7 ± 1.2	-5.6 ± 0.9	-3.0
65	-1297358.8 ± 1.6	-1297351.5 ± 0.0	7.3 ± 1.6	8.9 ± 1.7	-6.5 ± 1.2	0.7
67	-519090.6 ± 3.7	-519081.8 ± 0.3	8.7 ± 3.7	3.3 ± 3.7	-2.4 ± 2.7	-1.3
68	-620960.8 ± 1.9	-620962.2 ± 2.2	-1.5 ± 2.9	-3.0 ± 2.9	2.2 ± 2.1	1.4
69	-685227.5 ± 2.1	-685224.0 ± 0.8	3.4 ± 2.3	-0.7 ± 2.3	0.5 ± 1.7	-1.3
70	-521069.6 ± 1.5	-521065.2 ± 0.5	4.4 ± 1.6	-4.7 ± 1.6	3.5 ± 1.2	1.6
71	-553215.8 ± 2.1	-553211.5 ± 1.4	4.3 ± 2.5	3.0 ± 2.6	-2.2 ± 1.9	-0.1
72	-495797.5 ± 1.1	-495793.7 ± 0.2	3.9 ± 1.2	-2.9 ± 1.2	2.1 ± 0.9	0.6
74	-604490.8 ± 1.8	-604489.8 ± 1.9	1.0 ± 2.6	15.1 ± 2.6	-11.1 ± 1.9	-1.9
75	-543834.5 ± 0.8	-543833.6 ± 1.5	0.9 ± 1.7	-3.9 ± 1.7	2.8 ± 1.3	-2.8
80	-426925.7 ± 3.2	-426925.8 ± 0.6	-0.1 ± 3.3	8.6 ± 3.3	-6.3 ± 2.4	-2.2
81	-553121.1 ± 0.8	-553117.2 ± 0.6	3.9 ± 1.0	6.5 ± 1.1	-4.8 ± 0.8	-2.2
82	-713957.5 ± 0.7	-713956.1 ± 0.7	1.4 ± 1.0	-10.1 ± 1.1	7.4 ± 0.8	2.5
83	-1753380.1 ± 2.6	-1753389.2 ± 5.1	-9.1 ± 5.7	-4.3 ± 5.8	3.1 ± 4.2	-1.9
84	-990773.3 ± 2.4	-990769.2 ± 1.1	4.2 ± 2.6	1.5 ± 3.0	-1.1 ± 2.2	0.0
85	-526183.5 ± 1.7	-526184.2 ± 1.1	-0.7 ± 2.0	9.1 ± 2.0	-6.7 ± 1.5	-2.2
86	-686407.0 ± 1.3	-686403.1 ± 0.8	3.8 ± 1.5	-6.5 ± 1.5	4.8 ± 1.1	0.7
88	-576957.5 ± 1.7	-576960.7 ± 1.3	-3.2 ± 2.2	2.5 ± 2.2	-1.9 ± 1.6	-1.9
90	-621657.4 ± 0.9	-621656.1 ± 0.9	1.3 ± 1.3	-2.2 ± 1.4	1.6 ± 1.0	0.8
				(kcal/mol)	(log)	
$\mathbf{R^2}$ [h]	0.1	0.1	0.0	0.4	0.4	
MSD [i]				0.7	-0.5	
MAD [j]				3.1	2.3	
RMSD [k]				4.1	3.0	

[a] Molecule number [b] Free energy difference between MM and QM/MM with BLYP/6-31G* in water [c] Free energy difference between MM and QM/MM with BLYP/6-31G* in cyclohexane [d] Correction of the transfer free energy from water to cyclohexane based on QM/MM with BLYP/6-31G* [e] Corrected transfer free energy from water to cyclohexane based on QM/MM with BLYP/6-31G* [f] Partition coefficient based on QM/MM with BLYP/6-31G*

[g] Experimental distribution coefficient [h] Coefficient of determination with respect to experimental logD [i] Mean signed deviation from experimental logD results [j] Mean absolute deviation from experimental logD results [k] Root mean square deviation from experimental logD results

Figure 3: Comparison of the MM results based on CGenFF (red) with the QM/MM results based on BLYP/6-31G*/TIP3P (blue). Standard deviations are indicated by dotted error bars. Ideal correspondence to experiment is indicated by the black diagonal line, while deviations of 2 kcal/mol from experiment are indicated by the gray dashed diagonal lines. Molecule 74 is outside of the plotting range.

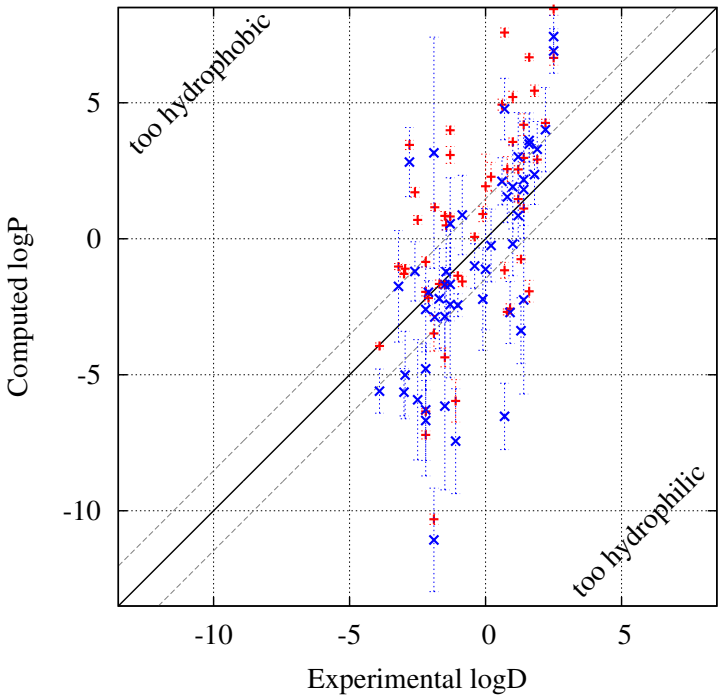

Table 2 and correspond to submission number 43. The solute was treated quantum-mechanically, while the solvent is treated classically via electrostatic embedding. A recent study demonstrated that this scheme can improve the RMSD of hydration free energies of selected molecules from 1.8 kcal/mol with CGenFF to 1.0 kcal/mol.[52]

In contrast to the previous findings, using QM/MM with BLYP for the solute does not lead to a significant improvement of the overall RMSD (4.1 kcal/mol compared to 4.4 kcal/mol with CGenFF — see last row). Interestingly, the mean signed deviation changes sign from MM to QM/MM (+0.7 compared to −1.2 kcal/mol— see third row from the bottom), which means that QM/MM is more hydrophilic than MM. Based on recent hydration

free energy calculations we expect that this increased hydrophilicity might be even more pronounced when employing hybrid density functional methods or MP2.[52] Given the relatively high computational costs of QM/MM calculations, the only very slight improvement of accuracy might appear discouraging. However, a casual glance at the standard deviations of the free energy correction ($\Delta\Delta A_{corr}^{BLYP}$, fourth column) reveals that most of the free energy results are not converged. The standard deviations range between 0.6 and 5.7 kcal/mol, with an average of 2.0 kcal/mol, and are often larger than the value of the correction itself. Thus, most of the QM/MM free energy corrections are not statistically significant. This is also highlighted by the direct comparison of the MM and QM/MM results in Figure 3, where most MM results (red) lie within the error bars of the QM/MM results (blue).

The standard deviations of the free energy corrections are similar in both water (second column) and cyclohexane (third column). While the average standard deviation in water is 1.5 kcal/mol, it is 1.1 kcal/mol in cyclohexane. This indicates that convergence is slightly slower in water due to the higher polarity of the environment. However, the remaining difficulties can probably be attributed to the basic differences between the MM and the QM energies surfaces, such as bonded terms.[25] Since the Zwanzig equation with exponential averaging was employed to connect the two energy surfaces, the resulting free energy estimates can contain large systematic errors that overshadow the errors from the underlying Hamiltonian.[107] Moreover, the potential energy differences between QM and MM can become very large due to the nucleus-electron interactions in QM, so the implementation of the Zwanzig equation must also ensure proper numerical stability.

An interesting feature of the comparison of the MM and QM/MM results in Figure 3 is the steeper slope of the results compared to experiment ($LogP^{MM} \approx 1.3LogD^{exp} + 1.0$ and $LogP^{BLYP} \approx 1.4LogD^{exp} - 0.3$). This means that hydrophilic compounds tend to be too hydrophilic and hydrophobic molecules are too hydrophobic in both MM and QM/MM. Accounting for solute polarization via BLYP/6-31G* does not seem to have a major impact on the slope. The exaggerated solvent affinity could be explained in multiple ways: a) the representation of the solute in one or both phases is incorrect e.g., too strong electrostatic interactions in the aqueous phase or too strong dispersion forces in the cyclohexane phase, b) some molecules could become more hydrophilic by the introduction of charges in protonizable groups (correcting for this effect would require experimental pK_a values), c) hydrophilic molecules can drag waters along into the apolar phase (microsol-

vation), d) molecules can be stabilized in unfavorable environments via di- or multimerization, e) there could also be a subtle systematic error in the experimental interpretation or setup, f) there is an unexpectedly high concentration of water in the apolar phase (however, experimental data suggests that the concentration of water in wet cyclohexane is only 1.5mM - which is comparable to the vapor phase),[108] g) the results could be affected by the simulation of the wrong tautomers (e.g., for molecules 50, 56, 83).

Analogous calculations were performed with the semi-empirical methods OM1, OM2, OM3, and PM3. The results are summarized in Table 3. Since there are only parameters for H, C, N, and O atoms for some of the methods, the data is restricted to a subset of 34 molecules. The data set is referred to as the "HCNO" data set. To save space in the table, we also restrict ourselves to the discussion of transfer free energies — especially since logDs can trivially calculated from the free energies by a multiplication by -1.37. We also omit the standard deviations of the MM and QM/MM results, since they are listed in the previous tables. To allow for a direct comparison to the CGenFF results (MM) and the BLYP results (QM), the respective data are also included in Table 3 (third and fourth column). Compared to the complete data set, the RMSDs of the MM and QM results increase by 0.6 kcal/mol to 5.0 and 4.7 kcal/mol, respectively. Since the errors actually increase by using this subset, it can be assumed that the subset is as challenging as the main set.

The RMSDs of the semi-empirical results range between 4.9 (PM3) and 7.1 kcal/mol (OM1). Thus, the quality of the multi-scale results is about equal to or worse than pure MM. However, the standard deviations indicate that the semi-empirical free energies are also not converged. For all semi-empirical results, the standard deviations range between 1.2 and 15.5 kcal/mol, with an average of 2.8 kcal/mol. An extreme example is molecule 83, which is also the largest molecule in the entire data set (117 atoms). Due to its high number of degrees of freedom, one would expect difficulties in the reweighting process. Indeed, the standard deviations of all semi-empirical methods lie around 7–8 kcal/mol for this molecule. Moreover, the errors for molecule 83 are significantly higher than for the rest of the data set. In the extreme case of OM1, the error amounts to more than 30 kcal/mol. This is symptomatic of a complete lack of phase space overlap in the Zwanzig equation.

To avoid errors that arise from convergence issues with the Zwanzig equation it is preferable to restrict the analysis to molecules with more or less

Table 3: Transfer free energies from water to cyclohexane, using several semi-empirical methods to treat the solute (data in kcal/mol). Due to the limited availability of parameters, only results for 34 molecules containing exclusively H, C, N, O atoms are shown.

Mol[a]	ΔA^{exp} [b]	MM	QM	OM3	OM2	OM1	PM3
4	-3.0	-5.8	-5.5	-3.0 ± 15.5	-2.6 ± 1.9	-4.5 ± 1.6	-8.0 ± 2.2
10	2.3	2.3	3.0	0.5 ± 3.0	3.4 ± 2.1	3.8 ± 1.5	1.0 ± 1.6
11	4.0	1.5	6.8	3.2 ± 2.8	7.8 ± 1.9	8.6 ± 2.6	2.7 ± 2.5
13	2.0	6.0	8.4	6.0 ± 3.8	8.0 ± 3.2	6.8 ± 3.3	0.3 ± 3.1
15	3.0	1.2	3.6	7.4 ± 2.5	5.4 ± 1.7	4.3 ± 1.8	1.6 ± 1.9
17	-3.4	-9.1	-9.4	-4.4 ± 2.7	-2.1 ± 3.1	-4.2 ± 3.6	-7.5 ± 2.9
19	-1.6	-3.5	-4.1	0.1 ± 2.7	0.8 ± 2.5	-3.7 ± 3.4	-7.9 ± 2.2
26	3.6	-2.3	1.6	1.8 ± 1.7	2.1 ± 1.7	-1.2 ± 1.4	-0.6 ± 2.3
27	2.6	-1.6	3.9	5.3 ± 3.0	0.6 ± 2.1	-0.1 ± 2.1	-0.4 ± 2.6
42	1.5	8.1	10.2	8.7 ± 3.3	8.2 ± 2.7	9.3 ± 3.7	3.5 ± 3.7
50	4.4	1.4	2.4	2.3 ± 2.6	2.2 ± 3.4	3.6 ± 3.6	-0.2 ± 2.1
55	2.0	-1.1	3.9	6.5 ± 2.4	5.1 ± 1.5	3.7 ± 1.7	-0.7 ± 1.4
56	3.4	-0.9	8.1	2.8 ± 2.7	1.4 ± 2.1	2.0 ± 1.5	1.2 ± 2.6
58	-1.1	3.7	-2.1	6.3 ± 4.0	3.6 ± 2.6	-0.5 ± 2.2	-2.6 ± 2.9
60	5.3	5.4	7.6	5.1 ± 2.2	6.1 ± 1.6	5.0 ± 2.1	-0.4 ± 1.9
61	2.0	-0.7	1.7	0.4 ± 1.9	-0.3 ± 1.2	0.2 ± 1.5	-3.3 ± 1.7
63	4.1	1.8	7.7	6.9 ± 1.8	6.9 ± 2.4	10.5 ± 2.4	3.1 ± 2.1
65	-1.0	1.6	8.9	11.1 ± 3.8	11.0 ± 5.6	7.6 ± 3.1	-2.0 ± 3.6
67	1.8	-5.4	3.3	1.4 ± 3.2	1.7 ± 3.4	-6.9 ± 2.6	-4.7 ± 2.4
68	-1.9	-1.5	-3.0	-3.1 ± 4.1	-3.6 ± 3.3	-2.6 ± 2.7	-6.8 ± 5.0
69	1.8	-4.2	-0.7	-5.5 ± 3.0	1.9 ± 3.8	-1.8 ± 1.8	-6.0 ± 2.8
70	-2.2	-9.1	-4.7	-9.5 ± 1.6	-5.9 ± 2.0	-12.3 ± 2.3	-9.8 ± 1.3
71	0.1	-1.2	3.0	4.3 ± 2.4	2.8 ± 3.1	1.5 ± 3.4	-4.5 ± 2.4
72	-0.8	-6.7	-2.9	-4.9 ± 1.5	-5.8 ± 1.9	-5.0 ± 1.3	-9.1 ± 1.4
74	2.6	14.1	15.1	15.8 ± 3.4	12.8 ± 3.1	15.4 ± 1.7	7.5 ± 2.3
75	3.8	-4.7	-3.9	-1.7 ± 2.4	-0.6 ± 3.3	-2.8 ± 2.1	-3.4 ± 2.9
80	3.0	8.7	8.6	10.2 ± 3.8	7.8 ± 3.0	8.6 ± 3.1	7.3 ± 4.7
81	3.0	2.7	6.5	11.9 ± 2.5	12.6 ± 3.3	7.4 ± 2.2	-1.2 ± 3.0
82	-3.4	-11.5	-10.1	-8.3 ± 2.0	-6.0 ± 2.4	-10.1 ± 1.9	-13.8 ± 1.9
83	2.6	4.7	-4.3	13.4 ± 6.7	24.9 ± 7.8	33.1 ± 8.4	11.3 ± 7.8
85	3.0	9.8	9.1	6.6 ± 2.9	8.2 ± 2.0	7.1 ± 1.7	4.7 ± 2.8
86	-1.0	-10.3	-6.5	-3.4 ± 2.9	-4.5 ± 2.7	-4.0 ± 2.9	-6.8 ± 2.2
88	2.6	5.8	2.5	7.0 ± 2.4	6.6 ± 1.9	4.0 ± 2.1	-0.5 ± 2.9
90	-1.1	-3.5	-2.2	-0.9 ± 2.9	-0.3 ± 3.4	-0.5 ± 3.8	-2.3 ± 4.0
R^2 [c]		0.4	0.5	0.3	0.3	0.3	0.5
MSD [d]		-1.4	0.7	1.6	2.2	1.1	-3.0
MAD [e]		4.2	3.7	4.2	4.1	4.6	4.3
RMSD [f]		5.1	4.8	5.4	5.8	7.2	5.0
R^{2*} [c]		0.6	0.7	0.5	0.5	0.6	0.8
MSD* [d]		-3.6	0.0	-0.3	0.3	-1.5	-4.5
MAD* [e]		4.3	3.0	3.4	2.9	3.9	4.7
RMSD* [f]		5.1	3.6	4.1	3.5	4.6	5.4

[a] Molecule number — molecules that are part of the "converged HCNO" subset are underlined. [b] Experimental transfer free energy between water and cyclohexane, where $\Delta A^{exp} = -2.303$ kT logD [c] Coefficient of determination with respect to ΔA^{exp} [d] Mean signed deviation from ΔA^{exp} [e] Mean absolute deviation from ΔA^{exp} [f] Root mean square deviation from ΔA^{exp} * Respective values for the 22 molecules with an average standard error of all semi-empirical results below 1 kcal/mol (i.e. molecules 10, 11, 15, 19, 26, 27, 55, 56, 60, 61, 63, 67, 69, 70, 71, 72, 75, 81, 82, 85, 86). This excludes molecules with extremely poor overlap between the MM and the SQM potential energy surface. In such cases, the poor convergence of the Zwanzig equation is most likely the main source of error.

converged free energy results. For this purpose, we provide data for a more "converged" subset of molecules (i.e., molecules 10, 11, 15, 19, 26, 27, 55, 56, 60, 61, 63, 67, 69, 70, 71, 72, 75, 81, 82, 85, 86). These 21 molecules are characterized by an average standard error of all semi–empirical methods below 1 kcal/mol (which corresponds to a standard deviation $\sigma < 3.1$ kcal/mol). Metrics for the additional subset are marked by an asterisk in Table 3 (see last four rows). The cut–off of 1 kcal/mol is admittedly arbitrary, but the experimental data range (between −3.4 and +5.3 kcal/mol) is preserved and the average value of the experimental data points is 1.4 instead of 1.2 kcal/mol. Thus, the data in the set is only marginally more hydrophilic. Moreover, the median experimental free energy difference is exactly the same for both sets with a value of 2.0 kcal/mol. The main effect is that the average molecular weight over the whole set decreases from 285 to 252 amu.

When comparing the "converged HCNO" data set with the "HCNO" data set, one can see that most metrics for the MM predictions do not change significantly. The RMSD increases from 5.0 to 5.1 kcal/mol, and the R^2 increases from 0.4 to 0.5. Only the MSD decreases from −1.4 to −3.6 kcal/mol, which indicates that the predictions are on average too hydrophobic. This can be partially attributed to the elimination of some of the relatively large polar molecules (e.g., molecules 83, 74 and 42), whose predictions tended to be significantly too hydrophilic. This is illustrated in Figure 4, where the excluded molecules are marked in turquoise (a negative logD indicates hydrophilicity). This might indicate that it is more difficult to achieve convergence for polar molecules.

In contrast to the MM results, the QM and semi-empirical metrics improve drastically upon elimination of the worst unconverged results. While the RMSDs initially ranged between 4.7 and 7.1 kcal/mol, they now range between 3.5 (OM2) and 5.4 kcal/mol (PM3). Based on this data, QM/MM and OMx/MM perform slightly better than MM (RMSDs of 3.6, 3.5-4.4 kcal/mol versus 5.1 kcal/mol). Interestingly, in terms of RMSD OM2 performs equally well as BLYP (RMSDs of 3.5 and 3.6 kcal/mol), which might make it appealing for future applications, since the computational costs are drastically lowered by the use of semi-empirical methods. Notably, this finding could also be an effect of selection bias. Therefore, further evidence is required to support this finding. However, the good performance of OMx is further illustrated by extensive recent benchmarks.[109]

The relatively large differences within the OMx family of semi-empirical methods are unexpected. The largest differences of the transfer free en-

Figure 4: Comparison of the distribution coefficient results based on the HCNO subset (combination of turquoise and red data) and the "converged" HNCO subset (red). The "converged" subset excludes predictions with standard errors larger than 1.0 kcal/mol. Ideal correspondence to experiment is indicated by the black diagonal line, while deviations of 2 kcal/mol from experiment are indicated by the gray dashed diagonal lines. Molecule 83 is outside of the plotting range for OM1 and OM2.

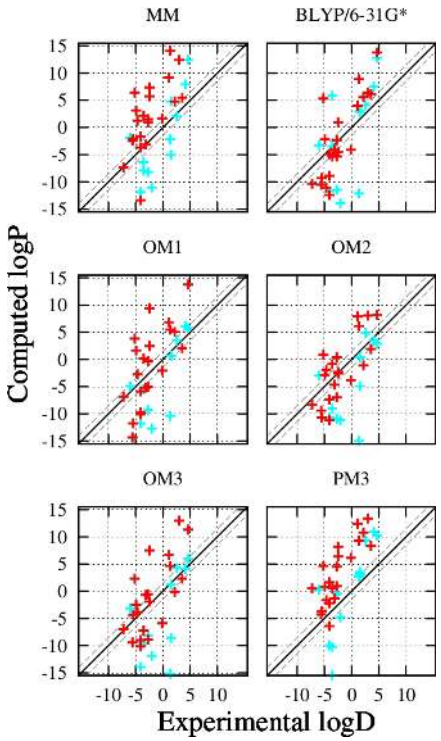

ergy between OM2 and OM3 in the "converged" set can be observed for molecule 69 (+7.4 kcal/mol), followed by molecules 27 (−4.7 kcal/mol), 11 (+4.7 kcal/mol) and molecule 70 (+3.6 kcal/mol). A common feature of those molecules is the presence of amines (cf. Fig. 1). However, it should be added that all molecules in the SAMPL5 challenge contain nitrogens, so this is not necessarily a unique feature. Nevertheless, a comparison of the net atomic charges of OM2 and OM3 reveals that the partial charges of carbons adjacent to nitrogen differ by between 0.05–0.07 e, with an average difference of 0.02 e over all 45 atoms. On the other hand, the charge response to the transfer from water to cyclohexane is similar. On average, the OM2 charges change by 0.0228 e, while the OM3 charges change by 0.0227 e upon transfer. Thus, the polarization response to the environment seems to be similar, but the initial partial charges differ.

For the interested reader, we also provide results for the semi-empirical methods AM1,[58] MNDO,[59] MNDO/d,[60] and MNDOC[61] in the Appendix. Their RMSDs range between 5.5 and 7.5 kcal/mol for the complete set, and 5.5 and 7.7 kcal/mol for the "converged" subset and tend to be significantly too hydrophobic (MSE between −0.9 and −3.5 kcal/mol or MSE* between −2.8 and −6.0 kcal/mol). The Appendix also contains data for OM2-D3, which uses the dispersion correction by Grimme et al.[48, 62, 110, 111] Even though such corrections only affect the intramolecular solute interactions, it seemed worthwhile to test their influence in view of the finding that the solvation free energy can be very conformation dependent.[112] However, the dispersion corrections do not change the results significantly (an RMSD* of 3.41 instead of 3.45 kcal/mol for the "converged" data set).

Table 4 lists the average computational costs of the different methods. On average, each MM transfer free energy result was obtained with ca. one year of CPU time (8952 CPU hours). This reflects the amount of time spent on equilibration as well as on each single λ point of the free energy calculation in both phases. The QM/MM post-processing with BLYP only required 16% of that time, since only the end points were used and only $\frac{1}{1000}$ of the total number of steps was analyzed (in order to decrease the auto-correlation between successive frames). For the semi-empirical methods with OMx and PM3, the additional computational costs amount to 0.06% of the costs of the standard free energy calculation. Considering that the corresponding calculations can also be trivially parallelized, the additional computational burden of the presented protocol is negligible.

Table 4: Average simulation time per molecule in CPU hours.

Method	CPU hours[a]	Relative computational time[b]
MM free energy calculations[c]	8952	100%
BLYP post-processing[d]	+1451	16.2%
OM3 post-processing[e]	+5	0.06%
OM2 post-processing[e]	+5	0.06%
OM1 post-processing[e]	+5	0.06%
PM3 post-processing[e]	+5	0.06%

[a] Average number of CPU hours spent on the computation for each molecule. This number does not account for the heterogeneity of the computer architectures. [b] Computational time relative to the full MM free energy calculations in percent. [c] Average simulation time per molecule, based on the complete data set, and including both equilibration and the simulation of all λ points of the free energy calculation. Simulations were performed on the LoBoS cluster (http://www.lobos.nih.gov). [d] Average time for the QM/MM post-processing per molecule, based on the complete data set — using 5000 data points in each phase. Calculations were performed on the Biowulf 1 computer cluster (http://hpc.nih.gov). [e] Average time for the semi-empirical SQM/MM post-processing per molecule. Calculations were performed on the Biowulf 1 computer cluster (http://hpc.nih.gov). (This represents an upper bound of the actual calculations, since the reported time is dominated by the cost of reading the CGenFF parameters and loading the PSF and structure, since each frame was treated independently.)

4. Conclusions

The explicit solvent calculations for the complete data set of 53 molecules indicate that QM/MM with BLYP/6-31G* performs similarly to MM with CGenFF (RMSDs of 4.1 and 4.4 kcal/mol, respectively). However, this comparison does not reflect the poor convergence of the Zwanzig equation when conducting multi-scale free energy calculations. By eliminating compounds with high standard deviations ($\sigma > 3.1$ kcal/mol, i.e. a standard error $>$ 1 kcal/mol), QM/MM appears more favorable than MM with an RMSD of 3.6 versus 5.1 kcal/mol for the HCNO data set. Under those restrictions, also semi-empirical methods perform well with RMSDs of 3.5 kcal/mol for OM2, 4.1 kcal/mol for OM3, 4.4 kcal/mol for OM1 and 5.4 kcal/mol for PM3. However, the possibility of some form of selection bias cannot be excluded in this case, since the relevant subset only contains 22 out of 53 molecules. Nevertheless, the data indicate that the inclusion of solute polarization improves the results.

With the possible exception of OM2, the MM, QM/MM and SQM/MM results exhibit a steeper slope than experiment. Since the solute charges and parameters vary among the different methods this suggests that the incline is not related to the solute parameters per se. All methods use TIP3P water and CGenFF cyclohexane as solvents, so this could be a possible reason for this behavior. Moreover, all solute–solvent interactions are based on the CGenFF Lennard Jones terms. The effect of different protonation states is discussed in our companion paper, but the pK_a corrections did.[63] Other possible explanations include microsolvation in the apolar phase, as well as di- and multimerization that can stabilize molecules in an unfavorable environment. Such effects will be the focus of our attention in the immediate future. Nevertheless, considering that an improvement of up to 30% of the RMSD can be achieved for 0.06% of extra costs, it is definitely worthwhile to employ semi-empirical theory for multi-scale free energy calculations. However, the problems of poor convergence and reliability of the free energy results still need to be addressed in a rigorous way before multi-scale techniques can become standard practice.

5. Acknowledgements

The authors would like to thank Tim Miller, Richard Venable and John Legato for technical assistance. We would also like to thank Richard Pastor

and Richard Venable for very helpful discussions concerning the nature of the apolar phase, especially in octanol. This work was partially supported by the intramural research program of the National Heart, Lung and Blood Institute of the National Institutes of Health and utilized the high-performance computational capabilities of the LoBoS and Biowulf Linux clusters at the National Institutes of Health. (http://www.lobos.nih.gov and http://hpc.nih.gov). The research leading to these results has also received funding from the European Research Council within an ERC Advanced Grant (OMSQC).

[1] M. Kah, C. D. Brown, LogD: Lipophilicity for ionisable compounds, Chemosphere 72 (10) (2008) 1401–1408. doi:10.1016/j.chemosphere.2008.04.074.

[2] J. Lee, B. T. Miller, B. R. Brooks, Computational scheme for pH-dependent binding free energy calculation with explicit solvent, Protein Sci. 25 (1, SI) (2016) 231–243. doi:10.1002/pro.2755.

[3] U. Ryde, P. Söderhjelm, Ligand-Binding Affinity Estimates Supported by Quantum-Mechanical Methods, Chem. Rev. 116 (9, SI) (2016) 5520–5566. doi:10.1021/acs.chemrev.5b00630.

[4] R. V. Stanton, D. S. Hartsough, K. M. Merz, Calculation of solvation free energies using a density functional/molecular dynamics coupled potential, J. Phys. Chem. 97 (1993) 11868–11870.

[5] M. R. Reddy, U. C. Singh, M. D. Erion, Development of a quantum mechanics-based free-energy perturbation method: use in the calculation of relative solvation free energies., J. Am. Chem. Soc. 126 (2004) 6224–5.

[6] M. R. Reddy, U. C. Singh, M. D. Erion, Ab initio quantum mechanics-based free energy perturbation method for calculating relative solvation free energies., J. Comput. Chem. 28 (2007) 491–4.

[7] D. Riccardi, P. Schaefer, Y. Yang, H. Yu, N. Ghosh, X. Prat-Resina, P. König, G. Li, D. Xu, H. Guo, M. Elstner, Q. Cui, Development of effective quantum mechanical/molecular mechanical (QM/MM) methods for complex biological processes., J. Phys. Chem. B 110 (2006) 6458–69.

[8] W. Yang, Q. Cui, D. Min, H. Li, Chapter 4 - QM/MM Alchemical Free Energy Simulations: Challenges and Recent Developments, Annu. Rep. Comput. Chem. 6 (2010) 51–62. doi:10.1016/S1574-1400(10)06004-4.

[9] W. Yang, R. Bitetti-Putzer, M. Karplus, Chaperoned alchemical free energy simulations: a general method for QM, MM, and QM/MM potentials., J. Chem. Phys. 120 (2004) 9450–3.

[10] D. Min, M. Chen, L. Zheng, Y. Jin, M. A. Schwartz, Q.-X. A. Sang, W. Yang, Enhancing QM/MM molecular dynamics sampling in explicit environments via an orthogonal-space-random-walk-based strategy., J. Phys. Chem. B 115 (2011) 3924–35.

[11] D. Min, L. Zheng, W. Harris, M. Chen, C. Lv, W. Yang, Practically Efficient QM/MM Alchemical Free Energy Simulations: The Orthogonal Space Random Walk Strategy, J. Chem. Theory Comput. 6 (2010) 2253–2266.

[12] J. Kästner, H. Senn, S. Thiel, N. Otte, W. Thiel, QM/MM free-energy perturbation compared to thermodynamic integration and umbrella sampling: Application to an enzymatic reaction, J. Chem. Theory Comput. 2 (2) (2006) 452–461. doi:10.1021/ct050252w.

[13] I. Polyak, T. Benighaus, E. Boulanger, W. Thiel, Quantum mechanics/molecular mechanics dual Hamiltonian free energy perturbation., J. Chem. Phys. 139 (2013) 064105–064116.

[14] H. M. Senn, W. Thiel, QM/MM methods for biomolecular systems., Ang. Chem. Int. Ed. 48 (2009) 1198–229.

[15] K. Nam, J. Gao, D. M. York, An Efficient Linear-Scaling Ewald Method for Long-Range Electrostatic Interactions in Combined QM/MM Calculations, J. Chem. Theory Comput. 1 (2005) 2–13.

[16] M. Štrajbl, G. Hong, A. Warshel, Ab Initio QM/MM Simulation with Proper Sampling: "First Principle" Calculations of the Free Energy of the Autodissociation of Water in Aqueous Solution, J. Phys. Chem. B 106 (51) (2002) 13333–13343. doi:10.1021/jp021625h.

[17] N. V. Plotnikov, S. C. L. Kamerlin, A. Warshel, Paradynamics: an effective and reliable model for ab initio QM/MM free-energy calculations and related tasks., J. Phys. Chem. B 115 (24) (2011) 7950–62. doi:10.1021/jp201217b.

[18] T. H. Rod, U. Ryde, Quantum Mechanical Free Energy Barrier for an Enzymatic Reaction, Phys. Rev. Lett. 94 (13) (2005) 138302. doi:10.1103/PhysRevLett.94.138302.

[19] T. H. Rod, U. Ryde, Accurate QM/MM Free Energy Calculations of Enzyme Reactions: Methylation by Catechol O-Methyltransferase, J. Chem. Theory Comput. 1 (6) (2005) 1240–1251. doi:10.1021/ct0501102.

[20] F. R. Beierlein, J. Michel, J. W. Essex, A Simple QM/MM Approach for Capturing Polarization Effects in Protein-Ligand Binding Free Energy Calculations, J. Phys. Chem. B 115 (17) (2011) 4911–4926. doi:10.1021/jp109054j.

[21] S. J. Fox, C. Pittock, C. S. Tautermann, T. Fox, C. Christ, N. O. J. Malcolm, J. W. Essex, C.-K. Skylaris, Free energies of binding from large-scale first-principles quantum mechanical calculations: application to ligand hydration energies, J. Phys. Chem. B 117 (32) (2013) 9478–9485. doi:10.1021/jp404518r.

[22] P. Mikulskis, D. Cioloboc, M. Andrejić, S. Khare, J. Brorsson, S. Genheden, R. A. Mata, P. Söderhjelm, U. Ryde, Free-energy perturbation and quantum mechanical study of SAMPL4 octa-acid host-guest binding energies, J. Comp.-Aid. Mol. Des. 28 (4, SI) (2014) 375–400. doi:10.1007/s10822-014-9739-x.

[23] S. Genheden, U. Ryde, P. Söderhjelm, Binding Affinities by Alchemical Perturbation Using QM/MM with a Large QM System and Polarizable MM Model, J. Comput. Chem. 36 (28) (2015) 2114–2124. doi:10.1002/jcc.24048.

[24] C. Sampson, T. Fox, C. S. Tautermann, C. Woods, C.-K. Skylaris, A "Stepping Stone" Approach for Obtaining Quantum Free Energies of Hydration, J. Phys. Chem. B 119 (23) (2015) 7030–7040. doi:10.1021/acs.jpcb.5b01625.

[25] G. König, B. R. Brooks, Correcting for the free energy costs of bond or angle constraints in molecular dynamics simulations, Biochim. Biophys. Acta - Gen. Subj. 1850 (5, SI) (2015) 932–943. doi:10.1016/j.bbagen.2014.09.001.

[26] C. Cave-Ayland, C.-K. Skylaris, J. W. Essex, Direct Validation of the Single Step Classical to Quantum Free Energy Perturbation, J. Phys. Chem. B 119 (3, SI) (2015) 1017–1025. doi:10.1021/jp506459v.

[27] M. A. Ollson, P. Söderhjelm, U. Ryde, Converging ligand-binding free energies obtained with free-energy perturbations at the quantum mechanical level, J. Comput. Chem. 37 (17) (2016) 1589–1600. doi:10.1002/jcc.24375.

[28] J. Gao, X. Xia, A priori evaluation of aqueous polarization effects through Monte Carlo QM-MM simulations., Science 258 (5082) (1992) 631–5.

[29] J. Gao, F. J. Luque, M. Orozco, Induced dipole moment and atomic charges based on average electrostatic potentials in aqueous solution, J. Chem. Phys. 98 (4) (1993) 2975. doi:10.1063/1.464126.

[30] V. Luzhkov, A. Warshel, Microscopic models for quantum mechanical calculations of chemical processes in solutions: LD/AMPAC and SCAAS/AMPAC calculations of solvation energies, J. Comput. Chem. 13 (2) (1992) 199–213. doi:10.1002/jcc.540130212.

[31] T. Wesolowski, A. Warshel, Ab Initio Free Energy Perturbation Calculations of Solvation Free Energy Using the Frozen Density Functional Approach, J. Phys. Chem. 98 (20) (1994) 5183–5187. doi:10.1021/j100071a003.

[32] J. Gao, M. Freindorf, Hybrid ab Initio QM/MM Simulation of N - Methylacetamide in Aqueous Solution, J. Phys. Chem. A 101 (17) (1997) 3182–3188. doi:10.1021/jp970041q.

[33] P. Kollman, Free energy calculations: Applications to chemical and biochemical phenomena, Chem. Rev. 93 (7) (1993) 2395–2417. doi:10.1021/cr00023a004.

[34] H. Li, W. Yang, Sampling enhancement for the quantum mechanical potential based molecular dynamics simulations: A general algorithm and its extension for free energy calculation on rugged energy surface., J. Chem. Phys. 126 (11) (2007) 114104. doi:10.1063/1.2710790.

[35] C. J. Woods, F. R. Manby, A. J. Mulholland, An efficient method for the calculation of quantum mechanics/molecular mechanics free energies., J. Chem. Phys. 128 (1) (2008) 014109. doi:10.1063/1.2805379.

[36] J. Heimdal, U. Ryde, Convergence of QM/MM free-energy perturbations based on molecular-mechanics or semiempirical simulations, Phys. Chem. Chem. Phys 14 (2012) 1259212604. doi:10.1039/c2cp41005b.

[37] H. Hu, Z. Lu, W. Yang, QM/MM Minimum Free Energy Path: Methodology and Application to Triosephosphate Isomerase., J. Chem. Theory Comput. 3 (2) (2007) 390–406. doi:10.1021/ct600240y.

[38] X. Zeng, H. Hu, X. Hu, A. J. Cohen, W. Yang, Ab initio quantum mechanical/molecular mechanical simulation of electron transfer process: fractional electron approach., J. Chem. Phys. 128 (12) (2008) 124510. doi:10.1063/1.2832946.

[39] H. Hu, Z. Lu, J. M. Parks, S. K. Burger, W. Yang, Quantum mechanics/molecular mechanics minimum free-energy path for accurate reaction energetics in solution and enzymes: sequential sampling and optimization on the potential of mean force surface., J. Chem. Phys. 128 (3) (2008) 034105. doi:10.1063/1.2816557.

[40] H. Hu, W. Yang, Elucidating solvent contributions to solution reactions with ab initio QM/MM methods., J. Phys. Chem. B 114 (8) (2010) 2755–9. doi:10.1021/jp905886q.

[41] G. König, F. C. Pickard, Y. Mei, B. R. Brooks, Predicting hydration free energies with a hybrid QM/MM approach: an evaluation of implicit and explicit solvation models in SAMPL4, J. Comput.-Aid. Mol. Design 28 (3, SI) (2014) 245–257. doi:10.1007/s10822-014-9708-4.

[42] G. König, P. S. Hudson, S. Boresch, H. L. Woodcock, Multiscale Free Energy Simulations: An Efficient Method for Connecting Classical MD Simulations to QM or QM/MM Free Energies Using Non-Boltzmann

Bennett Reweighting Schemes, J. Chem. Theory Comput. 10 (4) (2014) 1406–1419. doi:10.1021/ct401118k.

[43] P. S. Hudson, H. L. Woodcock, S. Boresch, Use of Nonequilibrium Work Methods to Compute Free Energy Differences Between Molecular Mechanical and Quantum Mechanical Representations of Molecular Systems, J. Phys. Chem. Lett. 6 (23) (2015) 4850–4856. doi:10.1021/acs.jpclett.5b02164.

[44] P. S. Hudson, J. K. White, F. L. Kearns, M. Hodošček, S. Boresch, H. L. Woodcock, Efficiently computing pathway free energies: New approaches based on chain-of-replica and Non-Boltzmann Bennett reweighting schemes, Biochim. Biophys. Acta - Gen. Subj. 1850 (5, SI) (2015) 944–953. doi:10.1016/j.bbagen.2014.09.016.

[45] T. Tuttle, W. Thiel, OMx-D: semiempirical methods with orthogonalization and dispersion corrections. implementation and biochemical application, Phys. Chem. Chem. Phys. 10 (2008) 2159–2166. doi:10.1039/B718795E.

[46] M. P. Repasky, J. Chandrasekhar, W. L. Jorgensen, PDDG/PM3 and PDDG/MNDO: Improved semiempirical methods, J. Comput. Chem. 23 (2002) 1601–1622.

[47] M. Elstner, D. Porezag, G. Jungnickel, J. Elsner, M. Haugk, T. Frauenheim, S. Suhai, G. Seifert, Self-consistent-charge density-functional tight-binding method for simulations of complex materials properties, Phys. Rev. B 58 (11) (1998) 7260–7268. doi:10.1103/PhysRevB.58.7260.

[48] P. O. Dral, X. Wu, L. Spörkel, A. Koslowski, W. Weber, R. Steiger, M. Scholten, W. Thiel, Semiempirical Quantum-Chemical Orthogonalization-Corrected Methods: Theory, Implementation, and Parameters, J. Chem. Theory Comput. 12 (3) (2016) 1082–1096. doi:10.1021/acs.jctc.5b01046.

[49] A. C. Simmonett, F. C. Pickard, H. F. Schaefer, III, B. R. Brooks, An efficient algorithm for multipole energies and derivatives based on spherical harmonics and extensions to particle mesh Ewald, J. Chem. Phys. 140 (18) (2014) 184101. doi:10.1063/1.4873920.

[50] A. C. Simmonett, F. C. Pickard, Y. Shao, T. E. Cheatham, III, B. R. Brooks, Efficient treatment of induced dipoles, J. Chem. Phys. 143 (7) (2015) 074115. doi:10.1063/1.4928530.

[51] A. S. Rustenburg, J. Dancer, B. Lin, D. F. Ortwine, D. L. Mobley, J. D. Chodera, Measuring experimental cyclohexane/water distribution coefficients for the SAMPL5 challenge, Same issue.

[52] G. König, Y. Mei, F. C. Pickard, A. C. Simmonett, B. T. Miller, J. M. Herbert, H. L. Woodcock, B. R. Brooks, Y. Shao, Computation of Hydration Free Energies Using the Multiple Environment Single System Quantum Mechanical/Molecular Mechanical Method, J. Chem. Theory Comput. 12 (1) (2016) 332–344. doi:10.1021/acs.jctc.5b00874.

[53] M. Kolb, W. Thiel, Beyond the MNDO model: Methodical considerations and numerical results, J. Comput. Chem. 14 (7) (1993) 775–789. doi:10.1002/jcc.540140704.

[54] W. Weber, W. Thiel, Orthogonalization corrections for semiempirical methods, Theor. Chem. Acc. 103 (6) (2000) 495–506. doi:10.1007/s002149900083.

[55] M. Scholten, Semiempirische Verfahren mit Orthogonalisierungskorrekturen: Die OM3 Methode, Ph.D. thesis, Heinrich-Heine-Universität Düsseldorf (2003).

[56] J. Stewart, Optimization of parameters for semiempirical methods I. Method, J. Comput. Chem. 10 (2) (1989) 209–220. doi:10.1002/jcc.540100208.

[57] K. E. Shaw, C. J. Woods, A. J. Mulholland, Compatibility of Quantum Chemical Methods and Empirical (MM) Water Models in Quantum Mechanics/Molecular Mechanics Liquid Water Simulations, J. Phys. Chem. Lett. 1 (1) (2010) 219–223. doi:10.1021/jz900096p.

[58] M. Dewar, E. Zoebisch, E. Healy, J. Stewart, AM1 - A New General Purpose Quantum Mechanical Molecular Model, J. Am. Chem. Soc. 107 (13) (1985) 3902–3909. doi:10.1021/ja00299a024.

[59] M. Dewar, W. Thiel, Ground states of molecules. 38. The MNDO method. Approximations and parameters, J. Am. Chem. Soc. 99 (15) (1977) 4899–4907. doi:10.1021/ja00457a004.

[60] W. Thiel, A. Voityuk, Extension of MNDO to d orbitals: Parameters and results for the second-row elements and for the zinc group, J. Phys. Chem. 100 (2) (1996) 616–626. doi:10.1021/jp952148o.

[61] W. Thiel, The MNDOC Method, a Correlated Version of the MNDO Model, J. Am. Chem. Soc. 103 (6) (1981) 1413–1420. doi:10.1021/ja00396a021.

[62] S. Grimme, J. Antony, S. Ehrlich, H. Krieg, A consistent and accurate ab initio parametrization of density functional dispersion correction (DFT-D) for the 94 elements H-Pu, J. Chem. Phys. 132 (15) (2010) 154104. doi:10.1063/1.3382344.

[63] F. C. Pickard, G. König, F. Tofoleanu, J. Lee, A. C. Simmonett, Y. Shao, J. W. Ponder, B. R. Brooks, Blind prediction of distribution in the SAMPL5 challenge with QM based protomer and pKa corrections, J. Comput.-Aid. Mol. Design.

[64] A. Nicholls, D. L. Mobley, J. P. Guthrie, J. D. Chodera, C. I. Bayly, M. D. Cooper, V. S. Pande, Predicting small-molecule solvation free energies: An informal blind test for computational chemistry, J. Med. Chem. 51 (4) (2008) 769–779. doi:10.1021/jm070549+.

[65] J. P. Guthrie, A Blind Challenge for Computational Solvation Free Energies: Introduction and Overview, J. Phys. Chem. B 113 (14) (2009) 4501–4507. doi:10.1021/jp806724u.

[66] A. V. Marenich, C. J. Cramer, D. G. Truhlar, Performance of SM6, SM8, and SMD on the SAMPL1 Test Set for the Prediction of Small-Molecule Solvation Free Energies, J. Phys. Chem. B 113 (14) (2009) 4538–4543.

[67] M. T. Geballe, A. G. Skillman, A. Nicholls, J. P. Guthrie, P. J. Taylor, The SAMPL2 blind prediction challenge: introduction and overview, J. Comput.-Aided Mol. Des. 24 (4, SI) (2010) 259–279. doi:10.1007/s10822-010-9350-8.

[68] P. V. Klimovich, D. L. Mobley, Predicting hydration free energies using all-atom molecular dynamics simulations and multiple starting conformations, J. Comput.-Aided Mol. Des. 24 (4, SI) (2010) 307–316. doi:10.1007/s10822-010-9343-7.

[69] A. Klamt, M. Diedenhofen, Blind prediction test of free energies of hydration with COSMO-RS, J. Comput. Aid. Mol. Des. 24 (4, SI) (2010) 357–360. doi:10.1007/s10822-010-9354-4.

[70] R. Ribeiro, A. Marenich, C. Cramer, D. Truhlar, Prediction of sampl2 aqueous solvation free energies and tautomeric ratios using the sm8, sm8ad, and smd solvation models, J. Comput. Aid. Mol. Des. 24 (4) (2010) 317–333.

[71] H. S. Muddana, C. D. Varnado, C. W. Bielawski, A. R. Urbach, L. Isaacs, M. T. Geballe, M. K. Gilson, Blind prediction of host–guest binding affinities: a new SAMPL3 challenge, J. Comput.-Aided Mol. Des. 26 (5) (2012) 475–487. doi:10.1007/s10822-012-9554-1.

[72] G. König, B. R. Brooks, Predicting binding affinities of host-guest systems in the SAMPL3 blind challenge: the performance of relative free energy calculations, J. Comput.-Aided Mol. Des. 26 (5) (2012) 543–550. doi:10.1007/s10822-011-9525-y.

[73] E. Gallicchio, R. M. Levy, Prediction of SAMPL3 host-guest affinities with the binding energy distribution analysis method (BEDAM), J. Comput.-Aided Mol. Des. 26 (5) (2012) 505–516. doi:10.1007/s10822-012-9552-3.

[74] M. Lawrenz, J. Wereszczynski, J. M. Ortiz-Sánchez, S. E. Nichols, J. A. McCammon, Thermodynamic integration to predict host-guest binding affinities , J. Comput.-Aided Mol. Des. 26 (5) (2012) 569–576. doi:10.1007/s10822-012-9542-5.

[75] D. L. Mobley, S. Liu, D. S. Cerutti, W. C. Swope, J. E. Rice, Alchemical prediction of hydration free energies for SAMPL, J. Comput.-Aided Mol. Des. 26 (5) (2012) 551–562. doi:10.1007/s10822-011-9528-8.

[76] M. T. Geballe, J. P. Guthrie, The SAMPL3 blind prediction challenge: transfer energy overview, J. Comput.-Aided Mol. Des. 26 (5, SI) (2012) 489–496. doi:10.1007/s10822-012-9568-8.

[77] O. Beckstein, B. I. Iorga, Prediction of hydration free energies for aliphatic and aromatic chloro derivatives using molecular dynamics simulations with the OPLS-AA force field, J. Comput.-Aided Mol. Des. 26 (5, SI) (2012) 635–645. doi:10.1007/s10822-011-9527-9.

[78] J. Reinisch, A. Klamt, M. Diedenhofen, Prediction of free energies of hydration with COSMO-RS on the SAMPL3 data set, J. Comput.-Aided Mol. Des. 26 (5, SI) (2012) 669–673. doi:10.1007/s10822-012-9576-8.

[79] D. L. Mobley, S. Liu, D. S. Cerutti, W. C. Swope, J. E. Rice, Alchemical prediction of hydration free energies for SAMPL, J. Comput.-Aided Mol. Des. 26 (5, SI) (2012) 551–562. doi:10.1007/s10822-011-9528-8.

[80] C. W. Kehoe, C. J. Fennell, K. A. Dill, Testing the semi-explicit assembly solvation model in the SAMPL3 community blind test, J. Comput.-Aided Mol. Des. 26 (5, SI) (2012) 563–568. doi:10.1007/s10822-011-9536-8.

[81] J. P. Guthrie, SAMPL4, A Blind Challenge for Computational Solvation Free Energies: The Compounds Considered, Same issue.

[82] D. L. Mobley, K. Wymer, N. M. Lim, Blind prediction of solvation free energies from the SAMPL4 challenge, Same issue.

[83] S. Genheden, Predicting Partition Coefficients with a Simple All-Atom/Coarse-Grained Hybrid Model, J. Chem. Theory Comput. 12 (1) (2016) 297–304. doi:10.1021/acs.jctc.5b00963.

[84] B. L. Tembe, J. A. McCammon, Ligand-receptor interactions, Comput. Chem. 8 (1984) 281–283.

[85] A. Villa, A. E. Mark, Calculation of the free energy of solvation for neutral analogs of amino acid side chains, J. Comput. Chem. 23 (2002) 548–553. doi:10.1002/jcc.10052.

[86] J. Maccallum, D. Tieleman, Calculation of the water-cyclohexane transfer free energies of neutral amino acid side-chain analogs using the OPLS all-atom force field, J. Comput. Chem. 24 (15) (2003) 1930–1935. doi:10.1002/jcc.10328.

[87] J. Michel, M. Orsi, J. W. Essex, Prediction of partition coefficients by multiscale hybrid atomic-level/coarse-grain simulations, J. Phys. Chem. B 112 (3) (2008) 657–660. doi:10.1021/jp076142y.

[88] B. Brooks, C. Brooks III, A. Mackerell Jr., L. Nilsson, R. Petrella, B. Roux, Y. Won, G. Archontis, C. Bartels, S. Boresch, A. Caflisch, L. Caves, Q. Cui, A. Dinner, M. Feig, S. Fischer, J. Gao, M. Hodošček, W. Im, K. Kuczera, T. Lazaridis, J. Ma, V. Ovchinnikov, E. Paci, R. Pastor, C. Post, J. Pu, M. Schaefer, B. Tidor, R. Venable, H. Woodcock, X. Wu, W. Yang, D. York, M. Karplus, CHARMM: The Biomolecular Simulation Program, J. Comput. Chem. 30 (10, Sp. Iss. SI) (2009) 1545–1614. doi:10.1002/jcc.21287.

[89] B. R. Brooks, R. E. Bruccoleri, B. D. Olafson, D. J. States, S. Swaminathan, M. Karplus, CHARMM: A program for macromolecular energy, minimization and dynamics calculations, J. Comput. Chem. 4 (1983) 187–217.

[90] K. Vanommeslaeghe, E. Hatcher, C. Acharya, S. Kundu, S. Zhong, J. Shim, E. Darian, O. Guvench, P. Lopes, I. Vorobyov, A. D. MacKerell, Jr., CHARMM General Force Field: A Force Field for Drug-Like Molecules Compatible with the CHARMM All-Atom Additive Biological Force Fields, J. Comp. Chem. 31 (4) (2010) 671–690. doi:10.1002/jcc.21367.

[91] C. H. Bennett, Efficient estimation of free energy differences from Monte Carlo data, J. Comp. Phys. 22 (1976) 245–268.

[92] W. L. Jorgensen, H. Chandrasekhar, J. D. Madura, R. W. Impey, M. L. Klein, Comparison of simple potential functions for simulating liquid water, J. Chem. Phys. 79 (1983) 926.

[93] E. Neria, S. Fischer, M. Karplus, Simulation of activation free energies in molecular systems, J. Chem. Phys. 105 (1996) 1902.

[94] T. Darden, D. York, L. Pedersen, Particle Mesh Ewald - An N.Log(N) method for Ewald sums in large systems, J. Chem. Phys. 98 (1993) 10089–10092.

[95] W. F. Van Gunsteren, H. J. C. Berendsen, Algorithms for macromolecular dynamics and costraint dynamics, Mol. Phys. 34 (1977) 1311–1327.

[96] Y. Sugita, A. Kitao, Y. Okamoto, Multidimensional replica-exchange method for free-energy calculations, J. Chem. Phys. 113 (2000) 6042.

[97] M. Zacharias, T. P. Straatsma, J. A. Mccammon, Separation-shifted scaling, a new scaling method for lennard-jones interactions in thermodynamic integration, J. Chem. Phys. 100 (1994) 9025.

[98] Y. Shao, L. F. Molnar, Y. Jung, J. Kussmann, C. Ochsenfeld, S. T. Brown, A. T. B. Gilbert, L. V. Slipchenko, S. V. Levchenko, D. P. O'Neill, R. A. DiStasio, Jr., R. C. Lochan, T. Wang, G. J. O. Beran, N. A. Besley, J. M. Herbert, C. Y. Lin, T. Van Voorhis, S. H. Chien, A. Sodt, R. P. Steele, V. A. Rassolov, P. E. Maslen, P. P. Korambath, R. D. Adamson, B. Austin, J. Baker, E. F. C. Byrd, H. Dachsel, R. J. Doerksen, A. Dreuw, B. D. Dunietz, A. D. Dutoi, T. R. Furlani, S. R. Gwaltney, A. Heyden, S. Hirata, C.-P. Hsu, G. Kedziora, R. Z. Khaliullin, P. Klunzinger, A. M. Lee, M. S. Lee, W. Liang, I. Lotan, N. Nair, B. Peters, E. I. Proynov, P. A. Pieniazek, Y. M. Rhee, J. Ritchie, E. Rosta, C. D. Sherrill, A. C. Simmonett, J. E. Subotnik, H. L. Woodcock, III, W. Zhang, A. T. Bell, A. K. Chakraborty, D. M. Chipman, F. J. Keil, A. Warshel, W. J. Hehre, H. F. Schaefer, III, J. Kong, A. I. Krylov, P. M. W. Gill, M. Head-Gordon, Advances in methods and algorithms in a modern quantum chemistry program package, Phys. Chem. Chem. Phys. 8 (27) (2006) 3172–3191. doi:10.1039/b517914a.

[99] H. L. Woodcock, III, M. Hodošček, A. T. B. Gilbert, P. M. W. Gill, H. F. Schaefer, III, B. R. Brooks, Interfacing Q-Chem and CHARMM to perform QM/MM reaction path calculations, J. Comp. Chem. 28 (9) (2007) 1485–1502. doi:10.1002/jcc.20587.

[100] W. Thiel, MNDO2005, version 7.1, Max-Planck-Institut für Kohlenforschung: Mülheim an der Ruhr, Germany, 2006.

[101] R. W. Zwanzig, High-temperature equation of state by a perturbation method. I. Nonpolar gases, J. Chem. Phys. 22 (1954) 1420.

[102] X. Jia, M. Wang, Y. Shao, G. König, B. R. Brooks, J. Z. H. Zhang, Y. Mei, Calculations of Solvation Free Energy through Energy Reweighting from Molecular Mechanics to Quantum Mechanics, J. Chem. Theory Comput. 12 (2) (2016) 499–511. doi:10.1021/acs.jctc.5b00920.

[103] E. C. Dybeck, G. König, B. R. Brooks, M. R. Shirts, A Comparison of Methods to Reweight from Classical Molecular Simulations to QM/MM Potentials, J. Chem. Theory Comput. 12 (4) (2016) 1466–1480. doi:10.1021/acs.jctc.5b01188.

[104] A. Becke, Density-functional exchange-energy approximation with correct asymptotic behavior, Phys. Rev. A 38 (6) (1988) 3098–3100. doi:10.1103/PhysRevA.38.3098.

[105] C. Lee, W. Yang, R. Parr, Development of the Colle-Salvetti correlation-energy formula into a functional of the electron density, Phys. Rev. B 37 (2) (1988) 785–789. doi:10.1103/PhysRevB.37.785.

[106] S. Piana, A. G. Donchev, P. Robustelli, D. E. Shaw, Water Dispersion Interactions Strongly Influence Simulated Structural Properties of Disordered Protein States, J. Phys. Chem. B 119 (16) (2015) 5113–5123. doi:10.1021/jp508971m.

[107] S. Bruckner, S. Boresch, Efficiency of Alchemical Free Energy Simulations I: Practical Comparison of the Exponential Formula, Thermodynamic Integration and Bennett's Acceptance Ratio Method, J. Comput. Chem. 32 (2011) 1303–1319.

[108] R. Wolfenden, A. Radzicka, On the probability of finding a water molecule in a nonpolar cavity, Science 265 (5174) (1994) 936–937. doi:10.1126/science.8052849.

[109] P. O. Dral, X. Wu, L. Spoerkel, A. Koslowski, W. Thiel, Semiempirical Quantum-Chemical Orthogonalization-Corrected Methods: Benchmarks for Ground-State Properties, J. Chem. Theory Comput. 12 (3) (2016) 1097–1120. doi:10.1021/acs.jctc.5b01047.

[110] S. Grimme, S. Ehrlich, L. Goerigk, Effect of the Damping Function in Dispersion Corrected Density Functional Theory, J. Comput. Chem. 32 (7) (2011) 1456–1465. doi:10.1002/jcc.21759.

[111] T. Risthaus, S. Grimme, Benchmarking of London Dispersion-Accounting Density Functional Theory Methods on Very Large Molecular Complexes, J. Chem. Theory Comput. 9 (3) (2013) 1580–1591. doi:10.1021/ct301081n.

[112] G. König, S. Boresch, Hydration Free Energies of Amino Acids: Why Side Chain Analog Data Are Not Enough, J. Phys. Chem. B 113 (26) (2009) 8967–8974. doi:10.1021/jp902638y.

6. Appendix

Table 5: Transfer free energies from water to cyclohexane, using the semi-empirical methods AM1, MNDO, MNDO/d, and MNDOC to treat the solute (data in kcal/mol). Due to the limited availability of parameters for some of the methods, only results for 34 molecules containing exclusively H, C, N, O atoms are shown.

Mol[a]	ΔA^{exp} [b]	MM	AM1	MNDO	MNDO/d	MNDOC
4	-3.0	-5.8	-0.7 ± 3.2	-5.6 ± 2.5	-7.4 ± 2.6	-7.6 ± 2.2
10	2.3	2.3	2.2 ± 2.1	1.4 ± 1.3	1.0 ± 1.7	-1.4 ± 1.6
11	4.0	1.5	15.4 ± 3.2	12.4 ± 2.6	11.2 ± 2.7	7.3 ± 2.6
13	2.0	6.0	-0.8 ± 4.2	2.3 ± 4.6	1.2 ± 3.9	2.3 ± 4.1
15	3.0	1.2	6.1 ± 2.9	2.7 ± 2.3	2.4 ± 2.8	3.7 ± 3.0
17	-3.4	-9.1	-1.0 ± 2.6	0.6 ± 3.6	-2.3 ± 3.7	-6.2 ± 3.8
19	-1.6	-3.5	-6.4 ± 2.0	-4.2 ± 2.3	-6.0 ± 2.7	-9.6 ± 3.0
26	3.6	-2.3	-2.4 ± 1.8	-4.0 ± 1.9	-4.2 ± 1.9	-2.5 ± 2.5
27	2.6	-1.6	2.8 ± 3.2	0.4 ± 2.0	-0.4 ± 2.9	-2.3 ± 2.6
42	1.5	8.1	2.7 ± 3.5	1.6 ± 4.5	1.7 ± 5.0	-1.8 ± 4.9
50	4.4	1.4	3.6 ± 4.2	2.5 ± 4.2	1.9 ± 5.0	-0.2 ± 4.4
55	2.0	-1.1	2.0 ± 2.0	0.0 ± 1.7	-1.3 ± 1.3	-0.3 ± 1.7
56	3.4	-0.9	1.3 ± 3.2	3.6 ± 3.1	1.4 ± 3.0	-1.8 ± 3.0
58	-1.1	3.7	0.6 ± 3.3	-5.9 ± 3.7	-8.1 ± 3.5	-9.3 ± 3.6
60	5.3	5.4	-0.5 ± 2.3	-0.5 ± 2.2	-0.8 ± 2.6	-1.4 ± 2.5
61	2.0	-0.7	-3.1 ± 1.6	-3.5 ± 1.9	-3.5 ± 2.5	-4.1 ± 3.1
63	4.1	1.8	1.7 ± 2.7	7.0 ± 3.1	6.0 ± 3.3	6.3 ± 3.9
65	-1.0	1.6	7.1 ± 3.8	4.6 ± 4.6	-3.0 ± 5.1	-6.9 ± 5.3
67	1.8	-5.4	-3.2 ± 2.6	-7.9 ± 2.5	-9.5 ± 3.0	-10.3 ± 3.5
68	-1.9	-1.5	-3.1 ± 4.5	-2.4 ± 3.2	-2.7 ± 3.7	-3.8 ± 3.5
69	1.8	-4.2	-6.6 ± 2.3	-4.6 ± 2.6	-6.6 ± 2.7	-5.8 ± 3.1
70	-2.2	-9.1	-7.1 ± 1.9	-11.3 ± 1.5	-12.4 ± 1.8	-13.0 ± 1.9
71	0.1	-1.2	-2.8 ± 2.0	-3.9 ± 2.3	-4.0 ± 3.7	-10.0 ± 3.4
72	-0.8	-6.7	-6.4 ± 1.8	-7.6 ± 2.1	-9.5 ± 2.3	-11.4 ± 1.9
74	2.6	14.1	5.9 ± 3.4	19.7 ± 3.2	19.4 ± 4.1	17.1 ± 4.2
75	3.8	-4.7	-5.1 ± 2.2	-7.8 ± 2.4	-8.0 ± 3.1	-12.8 ± 2.8
80	3.0	8.7	4.3 ± 3.3	7.7 ± 3.5	7.7 ± 3.8	8.4 ± 4.5
81	3.0	2.7	3.9 ± 2.1	2.5 ± 2.7	1.3 ± 2.6	-2.5 ± 2.2
82	-3.4	-11.5	-11.0 ± 2.4	-7.9 ± 3.0	-10.2 ± 3.2	-11.6 ± 3.5
83	2.6	4.7	19.2 ± 9.2	18.2 ± 13.4	17.0 ± 15.1	19.4 ± 16.1
85	3.0	9.8	5.7 ± 3.5	4.5 ± 2.2	4.4 ± 2.6	3.2 ± 2.8
86	-1.0	-10.3	-8.4 ± 1.9	-5.5 ± 2.4	-6.3 ± 3.2	-8.4 ± 3.3
88	2.6	5.8	0.6 ± 1.9	3.7 ± 2.6	3.7 ± 3.1	3.7 ± 3.5
90	-1.1	-3.5	-2.4 ± 3.3	-0.8 ± 2.9	-3.0 ± 3.2	-0.4 ± 3.5
$\mathbf{R^2}$[c]		0.4	0.2	0.2	0.3	0.3
MSD[d]		-1.4	-0.9	-1.0	-2.1	-3.5
MAD[e]		4.2	4.1	4.6	5.0	6.1
RMSD[f]		5.1	5.5	6.2	6.5	7.5
$\mathbf{R^{2*}}$[c]		0.6	0.5	0.4	0.5	0.5
MSD*[d]		-3.6	-2.8	-3.4	-4.4	-6.0
MAD*[e]		4.3	4.5	4.6	5.4	6.6
RMSD*[f]		5.1	5.5	5.7	6.3	7.7

[a] Molecule number — molecules that are part of the "converged HCNO" subset are underlined. [b] Experimental transfer free energy between water and cyclohexane, where $\Delta A^{exp} = -2.303\ kT\ logD$ [c] Coefficient of determination with respect to ΔA^{exp} [d] Mean signed deviation fromΔA^{exp} [e] Mean absolute deviation from ΔA^{exp} [f] Root mean square deviation from ΔA^{exp} * Respective values for the 22 molecules with an average standard error of all semi-empirical results below 1 kcal/mol (i.e. molecules 10, 11, 15, 19, 26, 27, 55, 56, 60, 61, 63, 67, 69, 70, 71, 72, 75, 81, 82, 85, 86). This excludes molecules with extremely poor overlap between the MM and the SQM potential energy surface. In such cases, the poor convergence of the Zwanzig equation is most likely the main source of error.

Table 6: Comparison of transfer free energies from water to cyclohexane, using the normal OM2 semi-empirical method (second column) and OM2 with D3 dispersion correction (OM2-D3, third column). Due to the limited availability of parameters for some of the methods, only results for 34 molecules containing exclusively H, C, N, O atoms are shown. All data in kcal/mol.)

Mol[a]	ΔA^{exp} [b]	OM2	OM2-D3	Difference
4	-3.0	-2.6 ± 1.9	-2.8 ± 2.0	0.20
10	2.3	3.4 ± 2.1	3.7 ± 2.3	-0.23
11	4.0	7.8 ± 1.9	7.1 ± 2.0	0.72
13	2.0	8.0 ± 3.2	7.8 ± 3.3	0.20
15	3.0	5.4 ± 1.7	5.2 ± 1.7	0.18
17	-3.4	-2.1 ± 3.1	-2.7 ± 3.0	0.68
19	-1.6	0.8 ± 2.5	0.4 ± 2.4	0.41
26	3.6	2.1 ± 1.7	2.0 ± 1.7	0.07
27	2.6	0.6 ± 2.1	0.9 ± 2.1	-0.25
42	1.5	8.2 ± 2.7	7.5 ± 2.7	0.70
50	4.4	2.2 ± 3.4	2.2 ± 3.4	0.04
55	2.0	5.1 ± 1.5	5.0 ± 1.5	0.08
56	3.4	1.4 ± 2.1	1.3 ± 2.0	0.09
58	-1.1	3.6 ± 2.6	3.6 ± 2.5	0.03
60	5.3	6.1 ± 1.6	6.2 ± 1.6	-0.13
61	2.0	-0.3 ± 1.2	-0.5 ± 1.3	0.21
63	4.1	6.9 ± 2.4	6.2 ± 2.4	0.66
65	-1.0	11.0 ± 5.6	10.9 ± 5.6	0.17
67	1.8	1.7 ± 3.4	1.2 ± 3.3	0.52
68	-1.9	-3.6 ± 3.3	-3.5 ± 3.3	-0.02
69	1.8	1.9 ± 3.8	2.0 ± 3.8	-0.07
70	-2.2	-5.9 ± 2.0	-6.0 ± 1.9	0.13
71	0.1	2.8 ± 3.1	3.6 ± 3.0	-0.76
72	-0.8	-5.8 ± 1.9	-5.4 ± 1.8	-0.36
74	2.6	12.8 ± 3.1	11.4 ± 3.1	1.39
75	3.8	-0.6 ± 3.3	-0.8 ± 3.2	0.23
80	3.0	7.8 ± 3.0	7.7 ± 3.0	0.13
81	3.0	12.6 ± 3.3	12.1 ± 3.2	0.46
82	-3.4	-6.0 ± 2.4	-6.5 ± 2.3	0.44
83	2.6	24.9 ± 7.8	20.3 ± 7.2	4.60
85	3.0	8.2 ± 2.0	8.3 ± 2.0	-0.09
86	-1.0	-4.5 ± 2.7	-5.0 ± 2.8	0.56
88	2.6	6.6 ± 1.9	5.4 ± 1.8	1.20
90	-1.1	-0.3 ± 3.4	-0.1 ± 3.6	-0.15
$\mathbf{R^2}$[c]		0.28	0.32	
MSD[d]		2.17	1.83	
MAD[e]		3.94	3.69	
RMSD[f]		5.75	5.11	
$\mathbf{R^{2*}}$[c]		0.54	0.55	
MSD*[d]		0.31	0.18	
MAD*[e]		2.77	2.79	
RMSD*[f]		3.45	3.41	

[a] Molecule number — molecules that are part of the "converged HCNO" subset are underlined. [b] Experimental transfer free energy between water and cyclohexane, where $\Delta A^{exp} = -2.303\ kT\ logD$ [c] Coefficient of determination with respect to ΔA^{exp} [d] Mean signed deviation from ΔA^{exp} [e] Mean absolute deviation from ΔA^{exp} [f] Root mean square deviation from ΔA^{exp} * Respective values for the 22 molecules with an average standard error of all semi-empirical results below 1 kcal/mol (i.e. molecules 10, 11, 15, 19, 26, 27, 55, 56, 60, 61, 63, 67, 69, 70, 71, 72, 75, 81, 82, 85, 86). This excludes molecules with extremely poor overlap between the MM and the SQM potential energy surface. In such cases, the poor convergence of the Zwanzig equation is most likely the main source of error.